Reviews

Vanadium Pentoxide Gels

J. Livage

Chimie de la Matière Condensée, Université Pierre et Marie Curie, 4 place Jussieu, 75252 Paris, France

Received December 3, 1990. Revised Manuscript Received May 28, 1991

Vanadium pentoxide gels have been known for more than a century. Fifty years ago they were used as models to study the hydrodynamic behavior of rodlike colloidal particles. Interest in them was renewed a decade ago by the discovery of their semiconducting properties and their use as antistatic coatings in the photographic industry. Since then vanadium pentoxide gels have been extensively studied by "sol-gel" scientists. They have a layered structure and give rise to anisotropic coatings when deposited onto a substrate. Such coatings exhibit a wide variety of electronic, ionic, and electrochemical properties. They behave as versatile host structures for the intercalation of ionic and molecular species and can be used for making humidity sensors, microbatteries, electrochromic display devices, and optical memories.

1. Introduction

The so-called "sol-gel process" has received significant attention during the past decade.[1] It offers new opportunities for the synthesis of glasses and ceramics. It is based on the hydrolysis and condensation of molecular precursors. The chemical control of these reactions allows the formation of monodispersed powders, thin films, or fibers directly from the solution at lower temperature than via the usual solid-state procedures.[2] Most papers are concerned with the sol-gel synthesis of silica and silica-based materials. Transition-metal oxides are also very important components in the ceramic industry. However, the high reactivity of the corresponding alkoxides makes the chemical synthesis of transition-metal oxide gels rather difficult.[3]

Vanadium pentoxide gels have been known for more than a century. They can be easily synthesized from both inorganic and metal-organic precursors and remain stable for months and even years when kept in a closed vessel. The fast growing development of the sol-gel process brought new interest in vanadium pentoxide gels. More than 100 papers on them have been published during the past decade, many patents have been taken, and some industrial applications appear promising. These gels exhibit a layered structure so that intercalation reactions have been extensively described.[4] They can lead to the synthesis of new organic-inorganic hybrid materials such as vanadium-polymer bronzes. $V_2O_5 \cdot nH_2O$ gels are actually composite materials made of solvent molecules (H_2O) trapped inside an oxide network (V_2O_5). They exhibit electronic properties arising from electron hopping through the mixed-valence oxide network as well as ionic properties arising from proton diffusion in the aqueous phase. Thin films can be easily deposited via the sol-gel process and vanadium pentoxide gels appear to be good candidates for microionic devices.[5]

2. Chemical Synthesis

Many synthesis of vanadium pentoxide sols or gels have already been reported in literature. The first one was described by Ditte in 1885.[6] He heated ammonium vanadate in a platinum crucible, then reacted the residue with hot nitric acid, and poured the mixture into water. He observed the formation of a red sol. Similar experiments using hydrochloric acid were published some years later by Biltz.[7] V_2O_5 sols have also been obtained via the thermohydrolysis of aqueous solutions of $VOCl_3$.[8] The hydrolysis and condensation processes of vanadium alkoxides $VO(OR)_3$ (R = Bu, *t*-Am) were already published at the beginning of the century.[9]

Vanadium pentoxide gels can also be made directly from the oxide. Hydrogen peroxide, for instance, reacts vigorously with crystalline V_2O_5, giving rise to a red gelatinous product.[10] Müller obtained vanadium pentoxide gels simply by pouring the molten oxide heated around 800 °C into water.[11] Large quantities of these gels are nowadays prepared this way for industrial purposes. More recently, it has been shown that hydration of amorphous V_2O_5 also leads to the formation of vanadium pentoxide gels.[12] The amorphous oxide was obtained by splat-cooling from the melt, and hydration was described as the swelling of a polymeric network into a solvent. Grinding the amorphous powder with water leads to the formation of gels and then sols as more and more water is added. Similar results have been observed with amorphous vanadium pentoxide films obtained by vapor deposition[13] or vanadium oxide spheres

(1) Brinker, C. J.; Scherrer, G. W. *Sol-gel Science*; Academic Press: San Diego, 1990.
(2) Klein, L. *Sol-gel technology*; Noyes Publications: Park Ridge, NJ, 1988.
(3) Livage, J.; Henry, M.; Sanchez, C. *Prog. Solid State Chem.* **1988**, *18*, 259.
(4) Aldebert, P.; Baffier, N.; Legendre, J. J.; Livage, J. *Rev. Chim. Miner.* **1982**, *19*, 485.
(5) Livage, J.; Barboux, P.; Badot, J. C. Baffier, N. Better Ceramics through Chemistry III. *Mater. Res. Soc. Symp. Proc.* **1988**, *121*, 167.
(6) Ditte, A. *C. R. Acad. Sci. Paris* **1885**, *101*, 698.
(7) Biltz, W. *Ber. Dtsch. Chem. Ges.* **1904**, *37*, 1098.
(8) Wegelin, G. *Z. Chem. Ind. Kolloide* **1912**, *11*, 25.
(9) Prandtl, W.; Hess, L. *Z. Anorg. Allg. Chem.* **1913**, *103*, 116.
(10) Ostermann, W. *Wiss. Ind. Hamburg* **1922**, *1*, 17.
(11) Müller, E. *Z. Chem. Ind. Kolloide* **1911**, *8*, 302.
(12) Gharbi, N.; R'Kha, C.; Ballutaud, D.; Michaud, M.; Livage, J.; Audiere, J. P.; Schiffmacher, G. *J. Non-Cryst. Solids* **1981**, *46*, 247.

0897-4756/91/2803-0578$02.50/0 © 1991 American Chemical Society

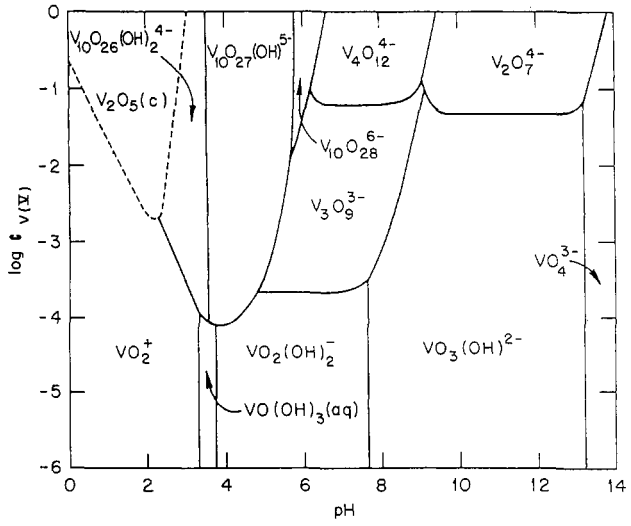

Figure 1. Predominant V(V) species in aqueous solutions at 25 °C as a function of vanadium concentration C and pH, according to ref 17.

formed by O_2–H_2 flame fusion.[14] These oxides readily dissolve into water, giving rise to gels or colloidal solutions. It has to be pointed out that crystalline vanadium pentoxide does not dissolve into water. Crystalline $V_2O_5 \cdot nH_2O$ hydrate have never been reported.[15] Hydration seems to be a unique property of the amorphous state even if vanadium pentoxide gels have been claimed to be obtained by grinding the crystalline powder for a long time in the presence of water.[16]

The most reliable synthesis methods for making vanadium pentoxide gels are based upon the hydrolysis and condensation of molecular precursors such as vanadates or vanadium alkoxides. Therefore we are going to give more details on these reactions.

a. Protonation of Vanadates in Aqueous Solutions. A large variety of V(V) species can be found in aqueous solutions. At room temperature they depend mainly on vanadium concentration and pH (Figure 1).[17] Main results in this field were obtained from combined potentiometric and ^{51}V NMR measurements by the Umea group.[18-20]

V(V) is a highly charged cation, so that oxo-anions $[VO_4]^{3-}$ in which vanadium is surrounded by four equivalent oxygen atoms are formed in highly alkaline aqueous solutions (pH > 14). Protonation occurs as the pH decreases, giving rise to hydrolyzed monomeric species $[H_nVO_4]^{3-n}$ in very diluted solutions ($c < 10^{-4}$ M). The mean negative charge of these anionic species decreases with the pH, as n increases, down to the point of zero charge (pH = 2). Below that pH value, monomeric cationic species $[VO_2]^+$ are observed.[17]

The situation is much more complex at higher concentration (Figure 2).[17,21] There is little doubt that monomeric orthovanadate $[VO_4]^{3-}$ remains the predominant species at very high pH. There is no evidence for condensed vanadates at pH = 14.[22] Condensation of the protonated $[HVO_4]^{2-}$ ion then occurs via oxolation, giving pyrovanadates $[V_2O_7]^{4-}$. Metavanadates such as $[V_4O_{12}]^{4-}$ are formed at lower pH. These polyanions form cycles or chains made of corner-sharing $[VO_4]^{3-}$ tetrahedra. Vanadium coordination increases up to six upon further condensation leading to the decavanadate ion $[V_{10}O_{28}]^{6-}$ and its protonated forms $[H_nV_{10}O_{28}]^{(6-n)-}$. The molecular structure of these isopolyvanadates was studied by ^{51}V and ^{17}O NMR in solutions or by X-ray diffraction when crystalline salts can be precipitated. It is now well-known and was reviewed recently.[21] Highly condensed species (gels or precipitates) are formed from neutral precursors such as $[VO(OH)_3]^0$. However such neutral monomeric species have never been found even for very low vanadium concentrations.[19,20] Vanadium atoms in these precursors would have a rather large positive partial charge ($\delta_V = +0.62$) so that coordination expansion occurs via the addition of nucleophilic species as follows:

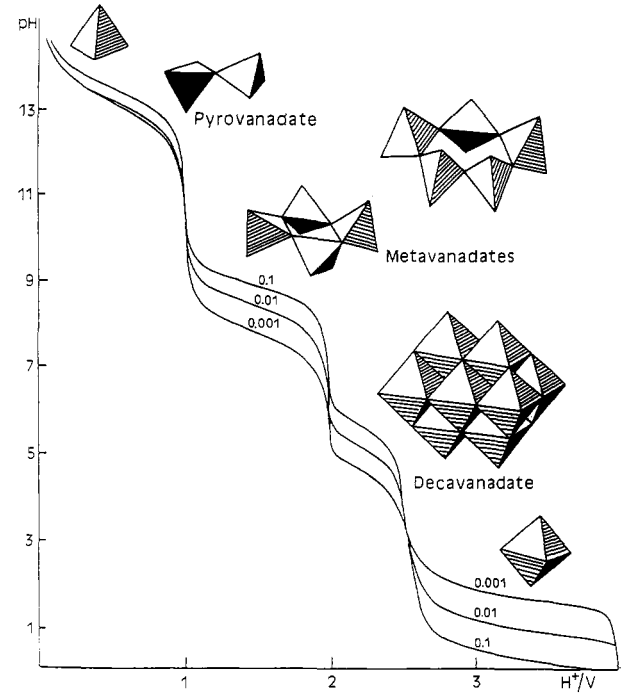

Figure 2. Structural evolution of V(V) aqueous species as a function of pH for different concentrations ranging from 10^{-3} to 10^{-1} mol L^{-1}.

(i) The nucleophilic addition of other neutral precursors $[VO(OH)_3]$ leads to the formation of decavanadic species between pH 2 and 6:

$$10[VO(OH)_3]^0 \rightarrow [H_6V_{10}O_{28}]^0 \rightarrow [H_2V_{10}O_{28}]^{4-} + 4H^+ + 12H_2O$$

Decavanadic species are strong acids. Spontaneous deprotonation occurs in water leading to pale yellow solutions of decavanadic acid $[H_2V_{10}O_{28}]^{4-}$ which appears to be the most protonated form of decavanadic species in aqueous solutions. Such polyanions cannot be precursors for more condensed species. OH groups give rise to acid dissociation and further condensation does not occur.

(ii) Water molecules are more nucleophilic than the neutral precursor. OH groups are more negatively charged ($\delta_{OH} = -0.2$) in H_2O than in $[VO(OH)_3]$ ($\delta_{OH} = -0.09$).[23]

(13) Sanchez, C.; Livage, J.; Audière, J. P.; Madi, A. *J. Non-Cryst. Solids* **1984**, *65*, 285.
(14) Kittaka, S.; Sasaki, S.; Ogawa, N.; Uchida, N. *J. Solid State Chem.* **1988**, *76*, 40.
(15) Théobald, F. *Bull. Soc. Chim. Fr.* **1975**, *7-8*, 1607.
(16) Wegelin, G. *Kolloid Z.* **1914**, *14*, 65.
(17) Baes, C. F.; Mesmer, R. E. In *The Hydrolysis of Cations*; Wiley: New York, 1976; p 197.
(18) Pettersson, L.; Hedman, B.; Andersson, I.; Ingri, N. *Chem. Scr.* **1983**, *22*, 254.
(19) Pettersson, L.; Hedman, B.; Nenner, A. M.; Andersson, I. *Acta Chem. Scand.* **1985**, *A39*, 499.
(20) Pettersson, L.; Andersson, I.; Hedman, B. *Chem. Scr.* **1985**, *25*, 309.
(21) Pope, M. T. In *Heteropoly and isopolymetallates*; Springer Publishers: Berlin, 1983.
(22) Heath, E.; Howarth, O. W. *J. Chem. Soc., Dalton Trans.* **1981**, 1105.

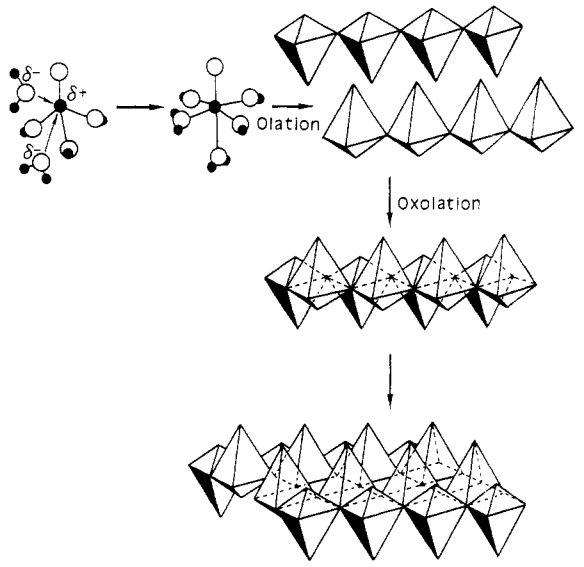

Figure 3. Possible condensation pathway leading to the formation of vanadium pentoxide gels from neutral $h = 5$ precursors $[VO(OH)_3]^0$ according to ref 3.

Therefore coordination expansion mainly occurs via water addition as follows:

$$[VO(OH)_3]^0 + 2H_2O \rightarrow [VO(OH)_3(OH_2)_2]^0$$

Vanadium becomes 6-fold coordinated with one water molecule along the z axis, opposite to the short V=O double bond, and another one in the equatorial plane, opposite to an OH group (Figure 3). Vanadium–oxygen bonds are not equivalent along x and y directions. Therefore condensation could occur more rapidly via olation along the H_2O–V–OH direction where both a good nucleophilic OH group ($\delta_{OH} = -0.14$) and an easily leaving water molecule ($\delta H_2O = +0.10$) are present:[23] This leads

$$H_2O\text{–}V(\overset{\delta-}{\text{–}}OH)\text{–}OH + H_2O\text{–}V(\overset{\delta+}{\text{–}}OH)\text{–}OH \longrightarrow H_2O\text{–}V\text{–}OH\text{–}V\text{–}OH + H_2O$$

to the formation of olated chain polymers (Figure 3). Slower oxolation reactions convert unstable $_2(OH)_1$ bridges into stable $_3(O)_1$ bridges, forming double chains. Further oxolation involving the last OH groups links these double chains together so that ribbonlike fibers are formed in agreement with electron microscopy observations (Figure 4).

Rapid association–dissociation equilibria have been observed in aqueous solutions. They mainly depend on vanadium concentration so that care has to be taken when dilution experiments are performed. Several condensed species are in equilibrium as follows:[24]

small oligomers ↔ high polymers ↔ colloids

Protonation is usually performed by adding an acid to aqueous solutions of vanadate salts.[6,7] It can be better performed via a proton exchange resin so that counteranions or -cations are removed from the solution.[25,26] Such a process is now currently used by many groups. The metavanadate aqueous solution is passed trough the resin. A pale yellow clear solution of decavanadic acid is first obtained. High polymers are then spontaneously formed. The solution becomes dark red, and its viscosity increases upon aging. Gelation occurs within a few hours when vanadium concentration is larger than 0.1 mol L^{-1}. It leads to a mixture of highly condensed polymeric fibers and decavanadic species, in agreement with the suggested condensation mechanism.[23,27] Colloidal species are negatively charged.[28] Protometric titration leads to about 0.2 negative charge per vanadium.[29]

b. Hydrolysis of Vanadium Alkoxides. Vanadium pentoxide gels can also be synthesized via the hydrolysis and condensation of vanadium oxoalkoxides $VO(OR)_3$ (R = Et, *n*-Bu, *n*-Pr, *i*-Pr, *t*-Am).[9] These alkoxides can be prepared upon heating under reflux a mixture of ammonium vanadate and alcohol as follows:

$$NH_4VO_3 + 3ROH \rightarrow [VO(OR)_3] + 2H_2O + NH_3$$

The reaction is carried out in benzene with an excess of alcohol. Water is eliminated via azeotropic distillation. The resulting alkoxide is purified by distillation under reduced pressure.

Physical and chemical properties of vanadium alkoxides depend on the nature of the alkoxy group.[30] They are all liquids, except $VO(OMe)_3$, which is a yellow crystalline solid. Its structure was resolved by X-ray diffraction.[31] It can be described as chain polymers made of edge-sharing distorted $[VO_6]$ octahedra with a short V=O bond and a long V–O bond along the z axis. Actually little is known about the molecular structure of vanadium alkoxides $VO(OR)_3$ in the liquid state. Cryoscopic measurements in cyclohexane suggest that bulky alkoxy groups (OR = O-*t*-Bu^t, O-*t*-Am) give rise to monomers, whereas oligomeric species are formed via alkoxy bridging with small primary alkoxides (OR = OEt, O-*n*-Pr, O-*n*-Bu).[32,33] However these alkoxy bridges are not very strong, so that oligomers are easily cleaved when dissolved into a solvent, leading to a mixture of monomers and oligomers. ^{51}V NMR spectra and X-ray absorption experiments at the vanadium K-edge were recently performed on liquid alkoxides.[34,35] They show that vanadium is tetrahedraly coordinated in monomers, and a square pyramidal coordination is observed in oligomeric species. In all cases a short V=O double bond about 1.6 Å long is observed.

Alcohol interchange reactions occur readily when vanadium alkoxides $VO(OR)_3$ are diluted in non-parent alcohols R'OH. They give rise to a mixture of $[VO(OR)_{3-x}(OR')_x]$ species.[30]

Vanadium alkoxides are very reactive toward hydrolysis. This arises from the high electrophilic power of the vanadium atom ($+0.4 < \delta_V < +0.5$) and the possible coordination expansion from 4 to 5 or 6. As for other alkoxides, hydrolysis rates decrease when the steric hindrance of alkoxy groups increases.[36] Therefore two parameters

(23) Henry, M.; Jolivet, J. P.; Livage, J. *Struct. Bonding*, in press.
(24) Von Ghosh, S.; Dhar, N. R. *Z. Anorg. Chem.* **1930**, *190*, 421.
(25) Hazel, J. F.; McNabb, W. M.; Santini, R. *J. Phys. Chem.* **1953**, *57*, 681.
(26) Lemerle, J.; Nejem, L.; Lefebvre, J.; *J. Inorg. Nucl. Chem.* **1980**, *42*, 17.
(27) Gharbi, N.; Sanchez, C.; Livage, J.; Lemerle, J.; Nejem, L.; Lefebvre, J. *Inorg. Chem.* **1982**, *21*, 2758.
(28) Zocher, Z. *Anorg. Chem.* **1925**, *147*, 91.
(29) Lemerle, J.; Nejem, L.; Lefebvre, J.; *J. Chem. Res., Miniprint* **1978**, *5*, 301.
(30) Bradley, D. C.; Mehrotra, R. C.; Gaur, D. P. In *Metal Alkoxides*; Academic Press: London, 1978.
(31) Caughlan, C. N.; Smith, H. M.; Watenbaugh, K. *Inorg. Chem.* **1966**, *5*, 2131.
(32) Lachowicz, V. A.; Höbold, W.; Thiele, K. H. *Z. Anorg. Allg. Chem.* **1975**, *418*, 65.
(33) Lachowicz, V. A.; Thiele, K. H. *Z. Anorg. Allg. Chem.* **1977**, *434*, 271.
(34) Sanchez, C.; Nabavi, M.; Taulelle, F. Better Ceramics through Chemistry III. *Mater. Res. Soc. Symp. Proc.* **1988**, *121*, 93.
(35) Nabavi, M.; Sanchez, C.; Verdaguer, M.; Michalowicz, A. *Inorg. Chim. Acta*, in press.
(36) Hirashima, H.; Tsukini, K.; Muratake, R. *J. Ceram. Soc. Jpn., Int. Ed.* **1989**, *97*, 232.

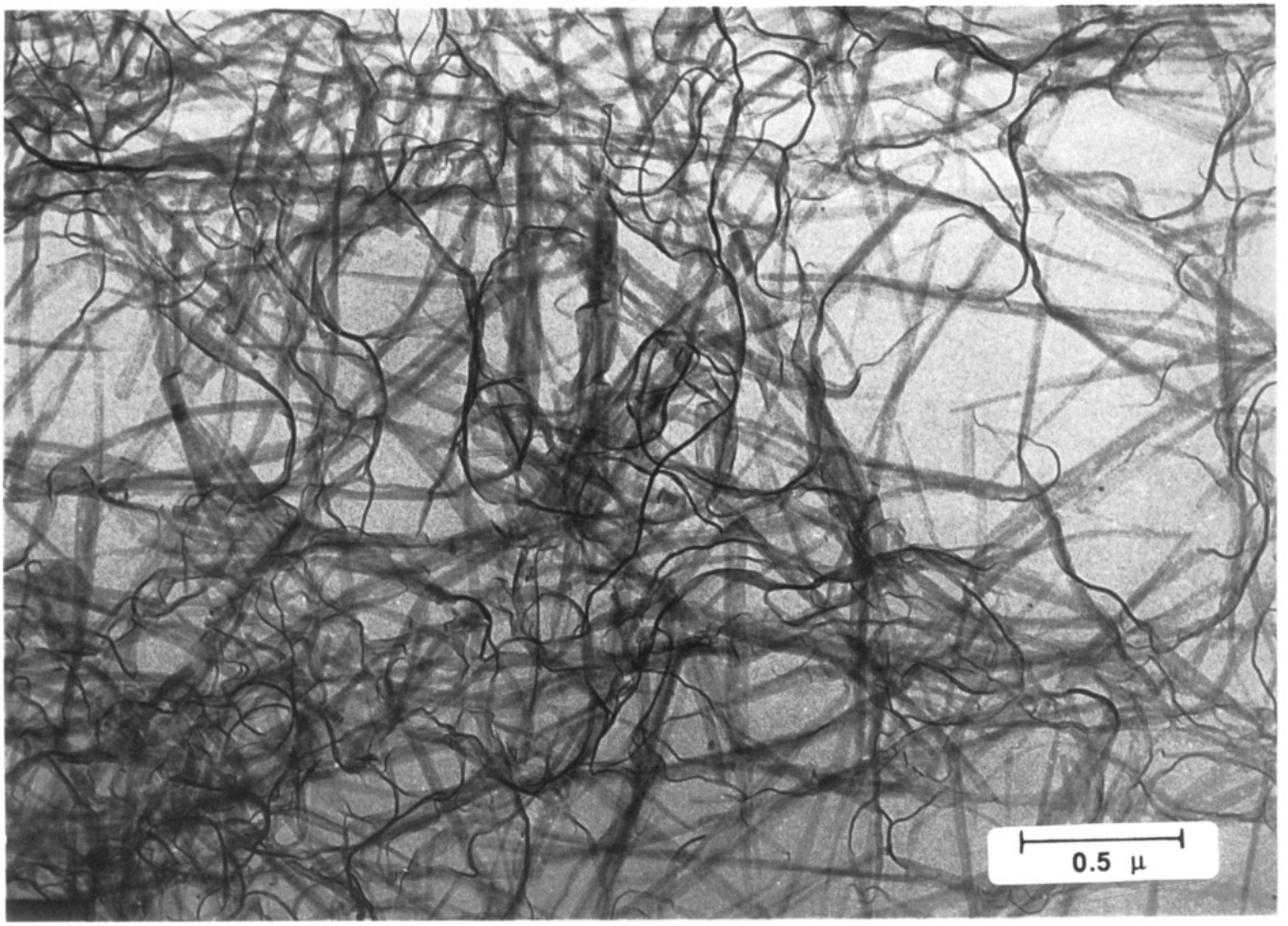

Figure 4. Electron microscopy showing the fibrous structure of vanadium pentoxide gels.

mainly control the formation of V_2O_5 gels: the hydrolysis ratio $h = (H_2O)/(V_2O_5)$ and the chemical nature of alkoxy groups.[37] The stoichiometric hydrolysis of a vanadium alkoxide would correspond to $h = 3$ as follows:

$$2VO(OR)_3 + 3H_2O \rightarrow V_2O_5 + 6ROH$$

Such a hydrolysis ratio leads to orange transparent gels with $VO(O\text{-}n\text{-}Pr)_3$ and colloidal solutions with $VO(O\text{-}t\text{-}Am)_3$. Red gels are obtained in both cases upon further hydrolysis ($h = 100$). However spontaneous reduction of vanadium by organic groups is observed with $VO(O\text{-}n\text{-}Pr)_3$ and gels become green.[34,37,38]

It appears that as hydrolysis proceeds, alkoxy ligands become band leaving groups so that they cannot be completely removed. Orange gels should then be described as polymeric alkoxo oxides $[V_2O_{5-x}(O\text{-}n\text{-}Pr)_x]_n$. Alkoxy ligands remain bonded to the oxide network. They can be removed only upon heating around 300 °C. SAXS experiments suggest that orange gels are made of highly branched polymeric species that still contain about 0.4 alkoxy group/vanadium as shown by thermal gravimetric analysis. X-ray absorption and ^{51}V NMR show that vanadium is in a distorted square-pyramidal ligand field. Such gels give transparent amorphous thin films.[34,38]

Molecular oligomers, about 10 Å in diameter, are obtained for low hydrolysis ratio ($h < 1$), while red gels are progressively formed within some hours in the presence of a large excess of water ($h > 100$). All alkoxy groups are then removed, and these red gels are very similar to those obtained from aqueous solutions. Electron microscopy shows that they are made of ribbonlike particles that give rise to anisotropic coatings when deposited onto a substrate. Moreover, acid dissociation of adsorbed water molecules occurs and molecular decavanadic species have been evidenced by ^{51}V NMR. Vanadium coordination is almost the same as in orange gels and crystalline V_2O_5, i.e., a 5-fold square-pyramidal coordination.[34,38]

Alkoxide precursors have been conveniently employed for the sol–gel synthesis of vanadium pentoxide based amorphous thin films (V_2O_5–TiO_2,[39,40,41] V_2O_5–GeO_2[42,43]) or crystalline vanadate compounds such as $NbVO_5$[44] or YVO_4.[45]

Some vanadium reduction always occurs during the synthesis of V_2O_5 gels from both alkoxides or aqueous solutions. It leads to the formation of V^{4+} species that are responsible for the mixed-valence properties of vanadium pentoxide gels.[27] The amount of V^{4+} ions is usually rather small (around 1%). However it can be larger than 10% when the synthesis is performed in an organic solvent.[37]

(37) Hioki, S.; Ohishi, T.; Takahashi, K.; Nakazawa, T. *J. Ceram. Soc. Jpn., Int. Ed.* **1989**, *97*, 617.
(38) Nabavi, M.; Sanchez, C.; Livage, J. *Eur. J. Inorg. Solid State Chem.*, in press.
(39) Hirashima, H.; Koyama, T.; Yoshida, T. *Yogyo-Kyokai-Shi* **1985**, *93*, 78.
(40) Hirashima, H.; Kamimura, S. *Mater. Res. Soc. Symp. Proc.* **1988**, *121*, 779.
(41) Hirashima, H.; Kamimura, S.; Muratake, R.; Yoshida, T. *J. Non-Cryst. Solids* **1988**, *100*, 394.
(42) Hou, L.; Sakka, S. *J. Non-Cryst. Solids* **1989**, *112*, 424.
(43) Hirashima, H.; Sudo, K. *J. Non-Cryst. Solids* **1990**, *121*, 68.
(44) Amarilla, J. M.; Casal, B.; Ruiz-Hitzky, E. *Mater. Lett.* **1989**, *8*, 132.
(45) Yamaguchi, O.; Mukaida, Y.; Shigeta, H.; Takemura, H.; Yamashita, M. *J. Electrochem. Soc.* **1989**, *136*, 1557.

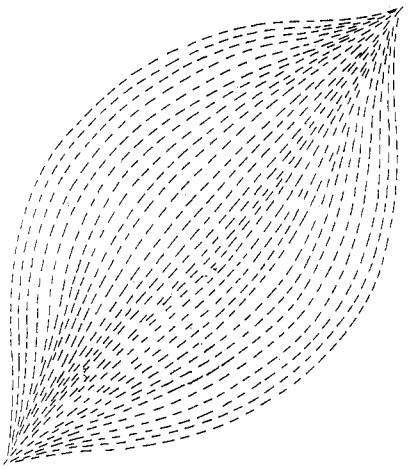

Figure 5. Schematic illustration of a spindlelike V_2O_5 tactoid.

V_2O_5 gels then turn green and flocculation occurs when the amount of reduced vanadium ions reaches 20%.[46] It seems that V^{4+} ions play an important role in the formation of V_2O_5 gels. They act as polymerization initiators.[26,27] This could be due to the weaker acidity of V^{4+}–OH groups compared to V^{5+}–OH ones. It could also arise from the bigger size of V^{4+} ions favoring coordination expansion,[47] which appears to be one of the most important parameter for the formation of condensed species from tetrahedrally coordinated inorganic or metal–organic precursors.[3]

3. Structure of Vanadium Pentoxide Gels

a. Layered Oxide Network. The fibrous structure of V_2O_5 colloids has been known for a long time.[48,49] Colloidal solutions of V_2O_5 become anisotropic when a shear stress or an electrical field are applied. Vanadium pentoxide sols have often been used as models to study the hydrodynamic behavior[50,5] or the optical birefringence[52] of anisotropic colloidal solutions. V_2O_5 sols are known to exhibit amazing properties such as thixotropy and rheopexy.[53,54]

Electron microscopy shows that $V_2O_5{\cdot}nH_2O$ gels are made of ribbonlike particles about 10 nm wide and over 1 μm long.[55] The growth process that leads to the formation of these fibers from vanadic acid aqueous solutions was recently investigated by cryogenic transmission electron microscopy.[56] Small threads, about 2 nm wide and 100 nm long, form first. They grow lengthwise, but subsequent self-assembly of these threads edge-to-edge leads to the formation of ribbonlike fibers, in agreement with the suggested condensation mechanism.[3]

The anisotropic shape of polymeric V_2O_5 particles leads to the formation of ordered colloidal phases called "tactoids".[57] Interactions between solid particles become rather strong in concentrated sols so that anisotropic colloids remain mutually oriented giving rise to spindlelike nematic tactoids with a major axis that can be as large as

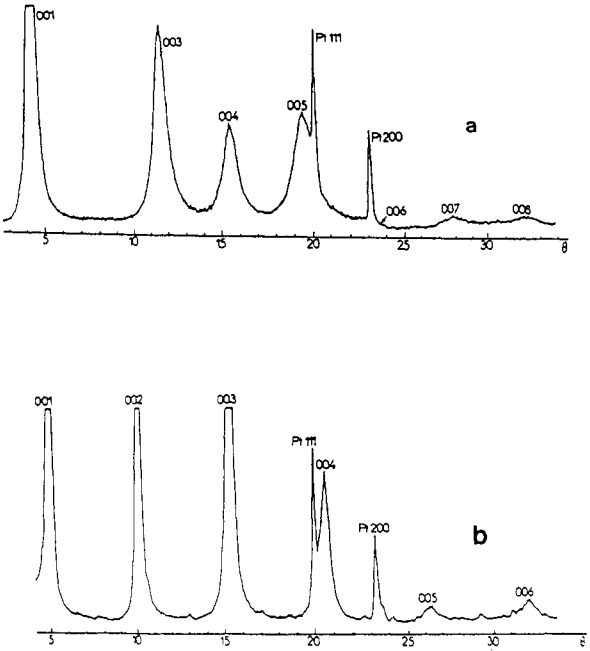

Figure 6. X-ray diffraction pattern of a $V_2O_5{\cdot}nH_2O$ layer deposited from a colloidal solution: (a) n = 1.8, basal distance d = 11.5 Å. (b) n = 0.5, basal distance d = 8.8 Å.

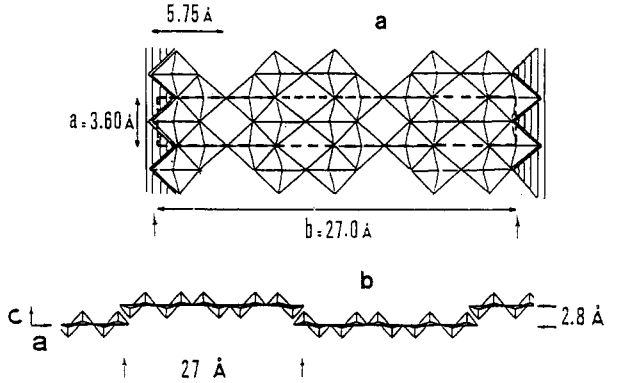

Figure 7. Structure of V_2O_5 ribbons: (a) Two-dimensional cell deduced from electron diffraction experiments. (b) Schematic cross section along the *ab* plane of the corrugated structure.

250 μm (Figure 5).[58] Such a spontaneous orientation can be preserved and even enhanced upon slow removal of the solvent. This leads to the formation of anisotropic coatings when vanadium pentoxide gels are deposited onto flat surfaces. An ordered stacking of the V_2O_5 ribbons is then observed leading to typical X-ray diffraction patterns (Figure 6).[59]

Two sets of X-ray diffraction patterns are actually observed,[59] a 00*l* one corresponding to the one-dimensional stacking of the ribbons perpendicular to the substrate and an *hk*0 one corresponding to the two-dimensional structure of the ribbons. The 00*l* set is observed on reflection patterns. The basal distance d depends on the amount of water in $V_2O_5{\cdot}nH_2O$ gels (Figure 6). The *hk*0 set is observed on X-ray diffraction transmission patterns and does not vary with n. Electron diffraction was performed on a single ribbon in order to obtain reliable indexation.[55] This leads to the following parameters of the 2-D cell: a = 27.0 Å and b = 3.6 Å (Figure 7a). This structure appears to be closely related to that observed in the *ab* plane of

(46) Babonneau, F.; Barboux, P.; Josien, F. A.; Livage, J. *J. Chim. Phys.* **1985**, *82*, 761.
(47) Nabavi, M.; Sanchez, C. *C. R. Acad. Sci. Paris* **1990**, *310*, 117.
(48) Donnet, J. B. *C. R. Acad. Sci. Paris* **1948**, 508.
(49) Takiyama, K. *Bull. Chem. Soc. Jpn., Int. Ed.* **1958**, *31*, 329.
(50) Donnet, J. B. *J. Chim. Phys.* **1953**, *50*, 291.
(51) Donnet, J. B.; Zbinden, H.; Benoit, H.; Daume, M.; Dubois, N.; Pouyet, J.; Scheibling, G.; Vallet, G. *J. Chim. Phys.* **1950**, *47*, 52.
(52) Errera, J.; Overbeek, J. Th.; Sack, H. *J. Chim. Phys.* **1935**, *32*, 681.
(53) Kistler, S. S. *J. Phys. Chem.* **1931**, *35*, 815.
(54) Juliusburger, F.; Pirquet, A. *Trans. Faraday Soc.* **1936**, 445.
(55) Legendre, J. J., Livage, J. *J. Colloid Interface Sci.* **1983**, *94*, 75.
(56) Bailey, J. K.; Nagase, T.; Pozarnsky, G. A.; MeCartney, M. L., Better Ceramics through Chemistry IV. *Mat. Res. Soc. Proc.* **1990**, *180*, 759.
(57) Heller, W. In *Polymer Colloids II*; Fitch, E., Ed.; Plenum Press: New York, 1980; p 153.
(58) Watson, J. H. L.; Heller, W.; Wojtowicz, W. *Science* **1949**, *109*, 274.
(59) Aldebert, P.; Baffier, N.; Gharbi, N.; Livage, J. *Mater. Res. Bull.* **1981**, *16*, 669.

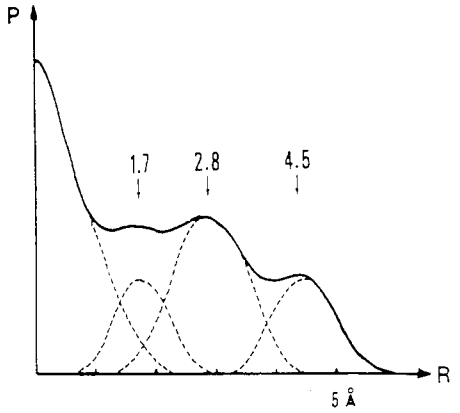

Figure 8. Patterson function calculated from 00*l* intensities diffracted by $V_2O_5 \cdot 1.8H_2O$ xerogels.

orthorhombic V_2O_5.[60] The *b* parameter is almost identical, but the *a* parameter is much larger (27 Å instead of 11.51 Å). This might be due to the presence of V–OH bonds that are removed only upon heating around 300 °C, just before the crystallization of orthorhombic V_2O_5.

A similar analysis of the X-ray diffraction pattern of several gels swelled with different solvents shows that the intensity of 00*l* peaks does not decrease regularly with the reciprocal interreticular distance. A common envelope can be drawn evidencing some systematic extinction of Bragg peaks around 0.17 and 0.50 $Å^{-1}$.[61] A monodimensional Patterson function was then calculated. It exhibits several broad maxima, the most important located around 2.8 Å (Figure 8). Such a shift can be attributed only to a nonplanar linkage between adjacent V_2O_5 units, leading to a corrugated ribbon structure (Figure 7b). The chemical nature of these links is not clear. They could be due to bridging OH groups or water molecules, but more experiments should be done in order to check this assumption.[174]

b. Intercalated Water Molecules. Hydrous oxide gels $V_2O_5 \cdot nH_2O$ are obtained upon hydrolysis and condensation of vanadium alkoxides or vanadates, i.e., in an aqueous medium. When dried under ambient conditions, the so-called xerogels contain about 1.8 H_2O per V_2O_5. Thermal analysis shows that water can be removed upon heating. Despite the fact that several authors[59,62] report a three-step process, it seems more reliable to describe the thermal water departure as follows:

$$V_2O_5 \cdot 1.8H_2O \xrightarrow{120\ °C} V_2O_5 \cdot 0.5H_2O \xrightarrow{250\ °C} V_2O_5$$

The corresponding enthalpies are close to $\Delta H_1 = 54$ kJ mol^{-1} and $\Delta H_2 = 65$ kJ mol^{-1}, respectively.[62] Amorphous vanadium oxide is then obtained above 250 °C. Crystallization into orthorhombic V_2O_5 occurs around 350 °C.[59]

Reversible water adsorption occurs at the oxide–air interface and the water content depends on the water pressure above the gel. The water adsorption isotherm (Figure 9) looks like a type II Brunauer gas–solid adsorption isotherm, suggesting a multilayer adsorption process.[63] The first water monolayer should be chemically bonded to the oxide network while the following ones would rather be physically adsorbed. The hydration state varies rather slowly ($1.4 < n < 1.9$) over a wide range of relative humidities around RH = 0.3. Stable gels corresponding to a rough formula $V_2O_5 \cdot 1.8H_2O$ are usually obtained under ambient conditions. Water adsorption remains reversible down to $n = 0.5$. Below this value water can no more be reversibly removed upon heating.[59]

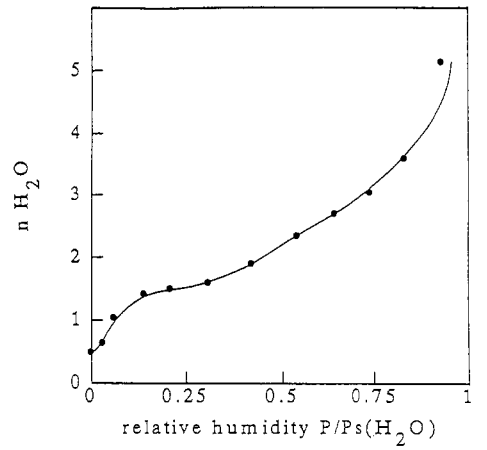

Figure 9. Water adsorption isotherm of $V_2O_5 \cdot nH_2O$ xerogels.

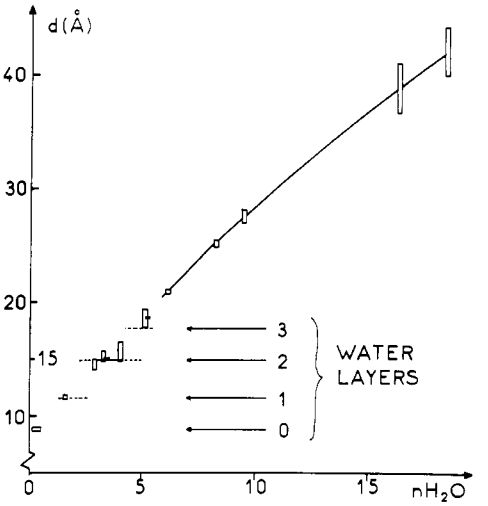

Figure 10. Variation of the basal distance *d* as a function of the hydration state of $V_2O_5 \cdot nH_2O$ gels.

According to the layered structure of $V_2O_5 \cdot nH_2O$ gels, water adsorption can actually be described as an intercalation process.[64,65] A one-dimensional swelling is observed by X-ray diffraction. The basal distance *d* increases by steps of about 2.8 Å corresponding to the van der Waals diameter of a water molecule (Figure 10). The smallest *d* value ($d = 8.8$ Å) corresponds to $n = 0.5$. It increases up to $d = 17.7$ Å ($n = 6$), suggesting that three water layers have been intercalated ($\Delta d = 7.9$ Å). Beyond this value, a continuous swelling mechanism takes place. Wide-angle neutron-scattering experiments show that the *d* spacing is then inversely proportional to the solid volume fraction in agreement with the 1-D swelling of large planar particles as was previously observed for sheet silicates such as montmorillonites.[64]

Small-angle X-ray (SAXS)[66] and neutron-scattering (SANS)[67] experiments show that scattered intensities do not follow the Porod law. An asymptotic h^{-2} decrease is

(60) Bachman, H. G.; Ahmed, F. R.; Barnes, W. H. *Z. Kristallogr.* **1961**, *115*, 110.
(61) Legendre, J. J.; Aldebert, P.; Baffier, N.; Livage, J. *J. Colloid Interface Sci.* **1983**, *94*, 84.
(62) Abello, L.; Pommier, C. *J. Chim. Phys.* **1983**, *80*, 373.
(63) Barboux, P.; Morineau, R.; Livage, J. *Solid State Ionics* **1988**, *27*, 221.
(64) Aldebert, P.; Haesslin, H. W.; Baffier, N.; Livage, J. *J. Colloid Interface Sci.* **1984**, *98*, 478.
(65) Kittaka, S.; Ayatsuka, Y.; Ohtani, K.; Uchida, N. *J. Chem. Soc., Faraday Trans. 1* **1989**, *85*, 3825.
(66) Kamiyama, T.; Itoh, T.; Suzuki, K. *J. Non-Cryst. Solids* **1988**, *100*, 466.
(67) Baffier, N.; Aldebert, P.; Livage, J.; Haesslin, H. W. *J. Colloid Interface Sci.* **1991**, *141*, 467.

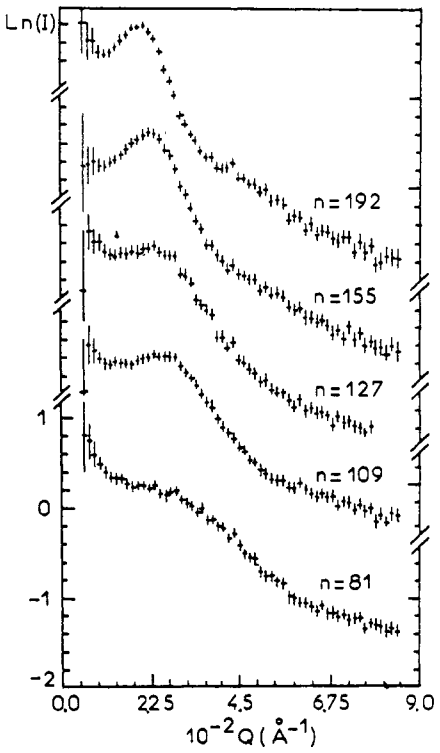

Figure 11. Small-angle neutron-scattering patterns of $V_2O_5{\cdot}nD_2O$ gels containing different amounts of D_2O.

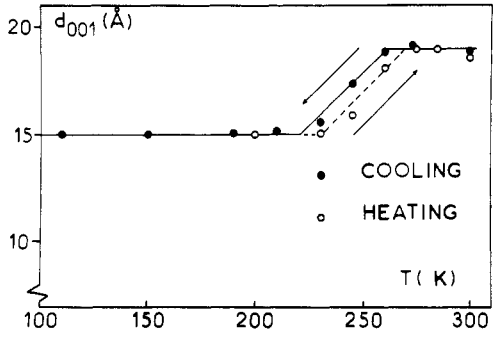

Figure 12. Temperature dependence of the position of the 00*l* peak deduced from neutron diffraction experiments performed on $V_2O_5{\cdot}6D_2O$ gels.

observed in the ln (I) vs ln (Q) plot, suggesting that V_2O_5 sols are made of Gaussian coils. However a Bragg peak appears to be superimposed to the scattering curve. Its position varies with the amount of water (Figure 11). It shifts toward smaller Q values (i.e., larger d spacing) when n increases. This means that spatial correlations between V_2O_5 ribbons already take place in colloidal solutions giving rise to ordered tactoids. Moreover the layered organization becomes gradually oriented parallel to the substrate as the water content decreases below n = 250. Some deviation from a typical random coil behavior is observed when the water content increases beyond n = 6000. Entangled ribbons should then be partially unravelled to form rods arising from the rotation of the ribbons around their main axis.[67]

Neutron diffraction and calorimetric measurements show that intercalated water molecules can be expelled from $V_2O_5{\cdot}nH_2O$ gels ($n > 5$) upon cooling.[62,68] The d spacing, measured from the position of the 00*l* line, first decreases below 0 °C and then remains constant (d = 15

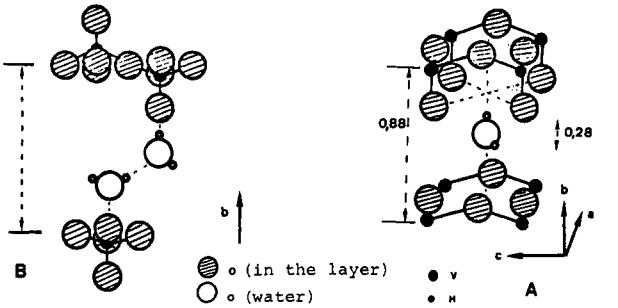

Figure 13. Position of water molecules in $V_2O_5{\cdot}nH_2O$ gels: (A) n = 0.5; (B) n = 1.8.

Å) down to 100 K (Figure 12). This suggests that two unfrozen water layers remain intercalated into the gel network while water in excess is expelled. This extra water begins to freeze around −20 °C, giving rise to the usual hexagonal form of ice. The process is reversible and expelled water molecules are intercalated again into the layered oxide network when temperature increases up to 300 K.

Infrared absorption and Raman spectroscopy performed on deuteriated gels show that the chemical nature of water molecules depends on the hydration state n in $V_2O_5{\cdot}nH_2O$.[69-73]

These experiments suggest that water molecules are very weakly hydrogen bonded to the oxide network when the xerogel is dried under vacuum (n = 0.5). Water molecules should then be trapped in some cavities between oxide layers.[72] Moreover, the antisymmetric stretching band ν_{OH} of HOD species exhibits a dichroic behavior. Therefore water molecules are not oriented at random. One of their O–H bonds must be perpendicular to the V_2O_5 ribbons as shown in (Figure 13a).[70]

The position and dichroic behavior of vibration bands in $V_2O_5{\cdot}1.8H_2O$ xerogels suggest that water molecules are linked together via hydrogen bonds.[73] Some of them have their C_{2v} axis perpendicular to the ribbons, whereas others are involved in hydrogen bonds with the V=O groups of the oxide network. The corresponding O–H bond is perpendicular to the ribbons (Figure 13b).[70]

Infrared and Raman spectra do not change significantly when the water content increases beyond n = 1.8. Intercalated water molecules are no more bonded to the oxide network. Dichroism of the $\nu_{V=O}$ band at 1020 cm^{-1} is lost beyond n = 6 when water intercalation turns into a continuous swelling process. An infrared spectrum corresponding to free water molecules is progressively obtained.[71]

Raman spectra of heated samples ($n < 0.5$) are very similar to those of crystalline V_2O_5 suggesting that vanadium oxide layers are linked via long V=O—O bonds as in the crystal.[72]

Dielectric relaxation experiments of $V_2O_5{\cdot}1.6H_2O$ xerogels were performed over a broad frequency range (10^4–10^{10} Hz).[74] They provide information about proton diffusion and the rotation of water molecules. The complex permittivity is expressed as $\epsilon^*(\omega) = \epsilon'(\omega) - i\epsilon''(\omega)$. The real

(68) Aldebert, P.; Haesslin, H. W.; Baffier, N.; Livage, J. *J. Colloid Interface Sci.* **1984**, *98*, 484.

(69) Sanchez, C.; Livage, J.; Lucazeau, G. *J. Raman Spectrosc.* **1982**, *12*, 68.

(70) Vandenborre, M. T.; Prost, R.; Huard, E.; Livage, J. *Mater. Res. Bull.* **1983**, *18*, 1133.

(71) Abello, L.; Lucazeau, G. *J. Chim. Phys.* **1984**, *81*, 539.

(72) Abello, L.; Husson, E.; Repelin, Y.; Lucazeau, G. *J. Solid State Chem.* **1985**, *56*, 379.

(73) Repelin, Y.; Husson, E.; Abello, L.; Lucazeau, G. *Spectrochim. Acta* **1985**, *41A*, 993.

(74) Badot, J. C.; Fourrier-Lamer, A.; Baffier, N. *J. Phys. (Paris)* **1985**, *46*, 2107.

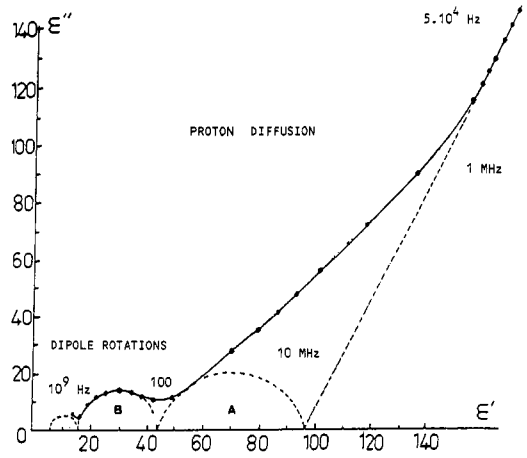

Figure 14. Cole–Cole diagram of a $V_2O_5 \cdot 1.8H_2O$ gel deduced from dielectric relaxation experiments at 300 K.

Table I. Exponential Variation of Dipole Rotation Relaxation Times $\tau = \tau_0 \exp(-W/kT)$ Deduced from Dielectric Relaxation Experiments in $V_2O_5 \cdot 1.8H_2O$

	τ_0, s	W, eV
circle A	3.10^{-14}	0.27
circle B	1.10^{-14}	0.21
circle C	7.10^{-15}	0.14
free H_2O	2.10^{-15}	0.22

part ϵ' corresponds to the dielectric permittivity and the imaginary part ϵ'' to dielectric losses. Measurements are often plotted as a so-called Cole–Cole diagram, $\epsilon'' = f(\epsilon')$. Two different parts can be seen (Figure 14). A straight line at low frequencies corresponds to the diffusion of charge carriers, and three semicircles at higher frequencies correspond to dielectric relaxations arising from the rotation of dipolar species. The corresponding Debye relaxation times τ, deduced from the top of these circles, follow an Arrhenius law $\tau = \tau_0 e^{-W/kT}$. Experimental values reported in Table I suggest that the first two circles, at lower frequencies, correspond to the rotation of water molecules strongly (circle a) and weakly (circle b) bonded to the oxide network. The third circle at high frequency could be assigned to the fast rotation of H_3O^+ species with a low activation energy (W = 0.14 eV). This last phenomenon actually disappears when protons are exchanged by Na^+ ions. Two other circles are observed in $Na_{0.33}V_2O_5 \cdot 1.6H_2O$ xerogels corresponding to the diffusion and intrasites jumps of Na^+ cations.[75]

c. Vanadium Coordination. The local structure of vanadium pentoxide gels made from vanadic acid was investigated by X-ray absorption experiments at the vanadium K-edge.[76-78] Polarized X-ray beams were used in order to take advantage of the strong anisotropy of $V_2O_5 \cdot 1.8H_2O$ layers. A large dichroism was actually found in both EXAFS and XANES spectra suggesting that vanadium sites are well oriented in the layer.[76,78] XANES experiments show that vanadium is in a square-pyramidal environment as in crystalline V_2O_5. The EXAFS signal for the z polarization is dominated by a single oscillation corresponding to the shortest V=O double bond (V–O = 1.58 Å, coordination number N = 1). Two other peaks can be observed in the Fourier transform of the absorption

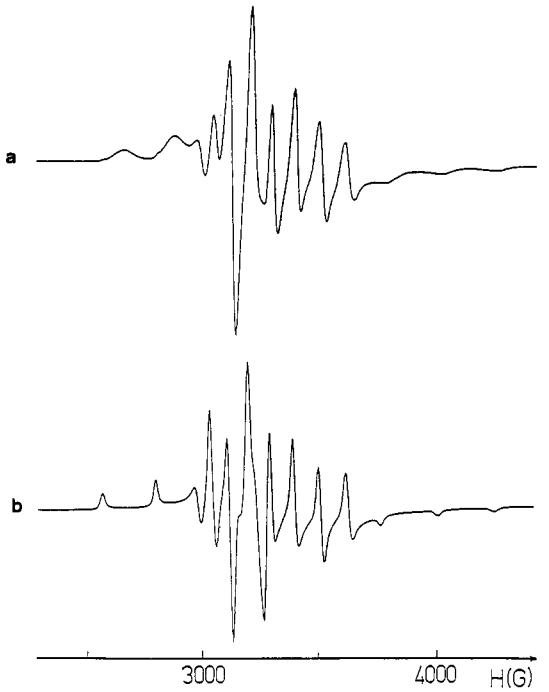

Figure 15. X-band ESR spectra of $V_2O_5 \cdot nH_2O$ gels recorded at 100 K: (a) n = 0.5; (b) n = 1.8.

Table II. ESR Parameters of $V_2O_5 \cdot n H_2O$ Xerogels and Reference Compounds

	$g_\parallel$	$g_\perp$	$A_\parallel$, G	$A_\perp$, G
$V_2O_5 \cdot 0.5H_2O$	1.925	1.982	196	76
$V_2O_5 \cdot 1.8H_2O$	1.935	1.986	204	78
V_2O_5	1.923	1.986	190	73
$[VO(H_2O)_5]^{2+}$	1.934	1.987	203	66

spectrum. The first one was assigned to a water molecule along the z axis, below the equatorial plane at a distance V–OH_2 = 2.7 Å. This water molecule should be rather weakly bonded to vanadium as suggested by the large Debye–Waller factor (σ^2 = 0.01 Å^2). The second peak is due to oxygen atoms of the nearest V=O group in the adjacent pyramid at a distance V–O = 3.7 Å. The EXAFS signal for E perpendicular to z is more complicated. It was analyzed as arising from two neighboring shells. The first one corresponds to four oxygen atoms in the equatorial plane, two at a distance of 1.87 Å, and the others at 1.78 and 2.02 Å as in crystalline V_2O_5. The second peak corresponds to three vanadium atoms in adjacent pyramids at a distance of about 3 Å.

Similar experiments were performed on red and orange gels obtained via the hydrolysis of vanadium alkoxides.[34,38,79] They show that in both cases vanadium is in a square-pyramidal [VO_5] environment with one short V=O bond of about 1.6 Å along the z axis. Moreover, two vanadium–vanadium distances are found corresponding respectively to edge sharing (V–V = 3.1 Å) and corner sharing (V–V = 3.3 Å) [VO_5] units.[34,38] Larger V–V distances (3.68 Å) were found in orange gels. They are probably due to the steric hindrance of the remaining alkoxy groups.

The ^{51}V solid-state NMR spectrum of red xerogels $V_2O_5 \cdot 1.8H_2O$ exhibits a broad peak around −280 ppm. According to the literature,[79] such a peak would correspond to V(V) in a square-pyramidal coordination with a mean V–O distance of about 1.83 Å.

(75) Badot, J. C.; Baffier, N. *Solid State Ionics* **1990**, *38*, 143.
(76) Stizza, S.; Benfatto, M.; Bianconi, A.; Garcia, J.; Mancini, G. Natoli, C. R. *J. Phys. (Paris)* **1986**, *47-C8*, 691.
(77) Stizza, S.; Davoli, I.; Benfatto, M. *J. Non-Cryst. Solids* **1987**, *95-96*, 327.
(78) Stizza, S.; Mancini, G.; Benfatto, M.; Natoli, C. R.; Garcia, J.; Bianconi, A. *Phys. Rev. B* **1989**, *40*, 12 229.
(79) Nabavi, M.; Taulelle, F.; Sanchez, C.; Verdaguer, M. *J. Phys. Chem. Solids* **1990**, *51*, 1375.

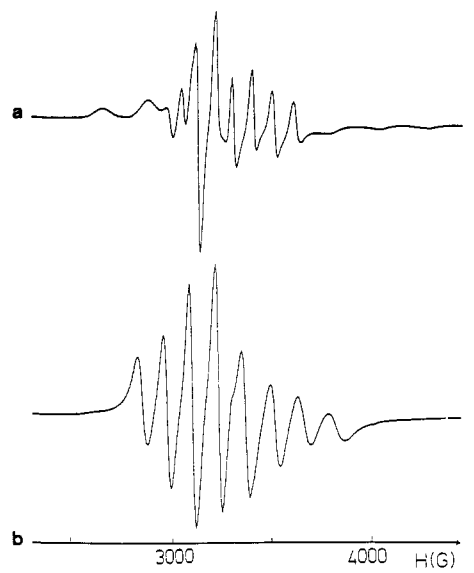

Figure 16. X-band ESR spectra of $V_2O_5 \cdot nH_2O$ gels recorded at room temperature: (a) $n = 0.5$; (b) $n = 1.8$.

Paramagnetic V(IV) ions are always present in vanadium pentoxide gels. They can be easily detected by ESR. The low-temperature ESR spectra of $V_2O_5 \cdot nH_2O$ xerogels (Figure 15) exhibit the typical hyperfine structure of localized V^{4+} ions ($S = {}^1/_2$, $I = {}^7/_2$) in an axially distorted crystal field. They can be described by the usual spin Hamiltonian:[80,81]

$$H = g_{\parallel}\beta H_z S_z + g_{\perp}\beta(H_x S_x + H_y S_y) + A_{\parallel} S_z I_z + A_{\perp} 1(S_x I_x + S_y I_y)$$

g and A values depend on the amount of water (Table II). The g tensor is similar to that of crystalline V_2O_5 when $n = 0.5$ (Figure 15a).[82] Hyperfine lines become sharper and ESR parameters become close to those of the solvated $[VO(H_2O)_5]^{2+}$ ion when $n = 1.8$ (Figure 15b).[83] This shows that water molecules belong to the coordination polyhedron of V(IV) ions giving rise to hydrated vanadyl species as evidenced by ENDOR spectroscopy.[81]

The ESR spectrum of $V_2O_5 \cdot 0.5H_2O$ does not change with temperature (Figure 16a) while $V_2O_5 \cdot 1.8H_2O$ powders give rise to an isotropic ESR spectrum at room temperature (Figure 16b). This isotropic spectrum ($g = 1.967$, $A = 117$ G) is due to the Brownian motion of paramagnetic species at the surface of the oxide network. Such a molecular tumbling at the oxide–water interface becomes possible as soon as water intercalation provides enough interlayer space for vanadyl ions to move.[84,85] These experiments suggest that V^{4+} ions are mainly localized at the surface of the oxide particles.

Vanadium pentoxide gels are very sensitive toward reduction. Even when left in open air, V_2O_5 layers progressively turn green after some weeks or months. Dehydration of $V_2O_5 \cdot nH_2O$ gels also leads to some reduction of vanadium ions.[86] Moreover the water content of a xerogel under a given water pressure increases when the reduction state increases.[87] Reduced xerogels ($V^{4+}/V^{5+} = 16\%$), in equilibrium with ambient atmosphere for instance, contain $2.5H_2O$ per V_2O_5 instead of 1.8 ($V^{4+}/V^{5+} = 1\%$). The internal structure of the oxide network does not change as long as the amount of reduced ions remains smaller than 20%. The 1-D stacking of the ribbons is preserved, but the basal distance increses up to 14.3 Å, suggesting the intercalation of another water layer.[88] These observations are not yet clearly understood. They could be due to a modification of the mean electronic charge of the oxide network arising from vanadium reduction. They more probably arise from the intercalation of reduced vanadyl VO^{2+} species solvated with two water layers.[87] These V^{4+} ions are presumably localized at the surface of the particles. They should not be involved in the vanadium pentoxide network and have not to be compensated by oxygen vacancies as in the crystalline material. It has to be pointed out that such a correlation between the reduced state of the gel and the amount of water could explain most discrepancies of literature. The amount of V^{4+}, the hydration state, and even the color of vanadium pentoxide gels are seldom given in most papers.

4. Electronic and Ionic Properties

Vanadium pentoxide gels or xerogels $V_2O_5 \cdot nH_2O$ are actually composite materials.[5] They contain water molecules trapped into an oxide network. Their physical properties then depend on the oxide phase, the liquid phase, and the interface between both phases. Water adsorption and dissociation occurs at the oxide–water interface so that vanadium pentoxide gels could be described either as hydrous oxides[89] $V_2O_5 \cdot nH_2O$ or poly(vanadic acids) $H_xV_2O_5 \cdot nH_2O$.[27] The amount of water can be measured by thermal analysis ($n \simeq 1.8$),[59] and acidity can be determined by protometric titration ($x \simeq 0.4$).[26]

a. Electrical Properties. The electrical properties of vanadium pentoxide gels have been extensively studied because of their potential application as semiconducting layers.[90] The antistatic coatings that are used in the photographic industry are based on silver-doped vanadia gels. They are made by heating V_2O_5 around 800 °C and pouring the molten oxide into water to form a colloidal solution. Layers deposited from these solutions exhibit rather low resistivity values (around 0.3 GΩ) and contain less than 10 mg of V_2O_5/m^2. One of the main interest of these antistatic coatings is that they are much less sensitive to humidity variations than other known antistatic materials.[91]

Many discrepancies can be found in literature about the electrical conductivity of vanadium oxide thin films deposited from gels. Room-temperature conductivities range from 10^{-6} to almost 1 Ω^{-1} cm^{-1}. Experimental values depend on many parameters such as the state of reduction of vanadium,[92,93] the relative humidity of the atmosphere,[94,95] and even the age of the gel or the thickness of

(80) Sanchez, C.; Babonneau, F.; Morineau, R.; Livage, J.; Bullot, J. *Philos. Mag. B* **1983**, *3*, 279.
(81) Barboux, P.; Gourier, D.; Livage, J. *Colloids Surf.* **1984**, *11*, 119.
(82) Sanchez, C.; Henry, M.; Grenet, J. C.; Livage, J. *J. Phys. C: Solid State* **1982**, *15*, 7133.
(83) Ballhausen, C. J.; Gray, H. B. *Inorg. Chem.* **1962**, *1*, 111.
(84) Sanchez, C.; Livage, J.; Tougne, P.; Legrand, A. P. *Magnetic Resonance in Colloids and Interface Science*; Fraissard, J., Resing, H., Eds.; Reidel: Dordrecht, 1980; p 559.
(85) Gharbi, N.; Sanchez, C.; Livage, J. *J. Chim. Phys.* **1985**, *82*, 755.
(86) Araki, B.; Audières, J. P.; Michaud, M.; Livage, J. *Bull. Soc. Chim. Fr.* **1981**, *9–10*, 366.
(87) Babonneau, F.; Barboux, P.; Josien, F. A.; Livage, J. *J. Chim. Phys.* **1985**, *82*, 761.
(88) Livage, J.; Barboux, P.; Tronc, E.; Jolivet, J. P. In *Science of Ceramic Chemical Processing*; Hench, L. L., Ulrich, D. R., Ed.; Wiley: New York, 1986; p 278.
(89) Slade, R. C. T.; Barker, J.; Halstead, T. K. *Solid State Ionics*, **1987**, *24*, 147.
(90) Guestaux, C.; French Patent 2,153,123, August 1971.
(91) Guestaux, C.; Leauté, J.; Virey, C.; Vial, J.; US Patent 3,658,573, April 1972.
(92) Barboux, P.; Baffier, N.; Morineau, R.; Livage, J. In *Solid State Protonic Conductors III*; Goodenough, J. B., Jensen, J., Potier, A., Eds.; Odense University Press: 1985; p 173.
(93) Bali, K.; Kiss, L. B.; Szörényi, T.; Török, M. I.; Hevesi, I. *J. Phys. (Paris)* **1987**, *48*, 431.

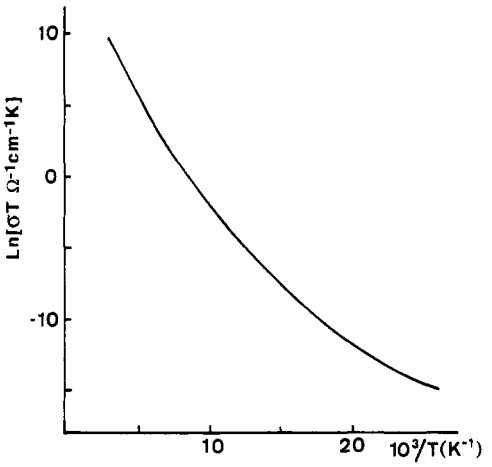

Figure 17. Temperature dependence of the electronic conductivity of a $V_2O_5 \cdot 0.5H_2O$ layer.

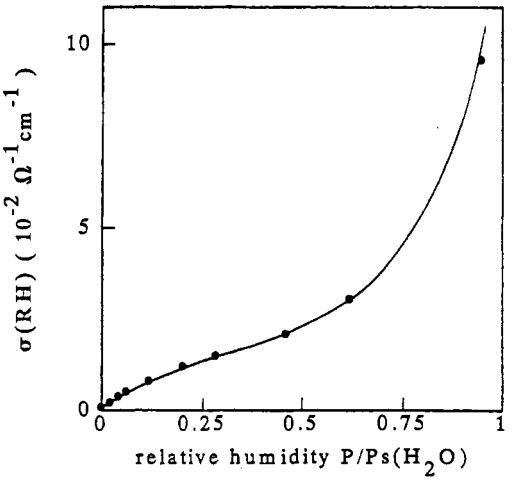

Figure 18. Room-temperature ac conductivity of a $V_2O_5 \cdot nH_2O$ layer as a function of the relative humidity.

the film.[96] Moreover, because of the layered structure of vanadium pentoxide gels, anisotropic conductivities are observed. Conductivity can be 4 orders of magnitude larger when measurements are performed in a direction parallel to the ribbons rather than perpendicular to them.[40]

Actually vanadium pentoxide gels are mixed conductors.[92] They exhibit both electronic and ionic conductivities so that care should be taken in order to separate both contributions. The overall electrical conductivity of $V_2O_5 \cdot nH_2O$ gels mainly depends on the hydration state n and the amount of reduced V^{4+} ions. The corresponding values should always be reported together with conductivity data. Both parameters appear to be related. Some reduction occurs when water is removed.[86] Hydration of $V_2O_5 \cdot nH_2O$ xerogels increases with the state of reduction.[87]

Electronic conduction prevails in dehydrated $V_2O_5 \cdot 0.5H_2O$ xerogels.[92,93,97] Nonstoichiometric vanadium pentoxide is a mixed-valence compound and its electronic properties arise from electron hopping between V^{4+} and V^{5+} ions.[98] It can be described by the so-called "small polaron model" as follows:[99]

$$\sigma T = \sigma_0 C(1 - C) \exp(-2\alpha R) \exp(-W/kT)$$

where C is the redox ratio ($C = V^{4+}/V^{4+} + V^{5+}$), α is the wave function decay, and R is the mean distance between vanadium ions.

Both the Seebeck and the Hall coefficients are negative, suggesting n-type charge carriers.[100] A strong electron–phonon coupling is observed, so that charge carriers have a rather low mobility, values ranging between 10^{-5} and 10^{-6} $cm^2\ V^{-1}\ s^{-1}$ are currently reported.[80] Room-temperature activation energies for conduction W range between 0.2 and 0.4 eV. However, the temperature dependence of conductivity does not follow an Arrhenius law.[101] The measured activation energy W is actually the sum of two terms, $W = W_h + W_d/2$ where W_h corresponds to a phonon-assisted hopping process and W_d to the structural disorder. This last term, measured in vanadium pentoxide gels, is close to 0.1 eV.[102] The thermal activation energy W_h decreases continuously with temperature as the phonon spectrum freezes out (Figure 17). According to theory,[99] a change in the conduction mechanism is expected at $T = \theta/2$. It was actually observed around 150 K.[103] The room-temperature dc conductivity is rather low. It increases with the state of reduction, from $4 \times 10^{-5}\ \Omega^{-1}\ cm^{-1}$ ($C = 1\%$) up to $2 \times 10^{-3}\ \Omega^{-1}\ cm^{-1}$ ($C = 10\%$).[92] The frequency dependence of electronic conductivity was discussed in terms of an overlapping polaron model,[104] and dc conductivity was analyzed in the frame of percolation theory.[105] Optically induced electron hopping gives an absorption band in the near infrared region around $h\nu = 1$ eV. This band shifts toward smaller energies as C increases.[106]

Ionic conduction in $V_2O_5 \cdot nH_2O$ prevails when $n > 0.5$. It arises from proton diffusion through the gel matrix.[107] Ac conductivity increases quite fast with the relative humidity. The $\sigma = f(P/P_s)$ curve has a sigmoid shape similar to that of the water adsorption isotherm (Figure 18). This suggests that proton diffusion mechanisms are related to the number of water molecules and the way they are adsorbed at the surface of the oxide framework.[92] At low water content ($n = 0.5$) water molecules are trapped inside cavities of the oxide network.[70] They cannot diffuse through the xerogel and are too far apart for protons to jump from one site to the other. Therefore electron hopping prevails, and the room-temperature ac conductivity is rather low, around $10^{-5}\ \Omega^{-1}\ cm^{-1}$. Ionic conductivity then increases as more water molecules are intercalated between V_2O_5 ribbons. A plateau is observed around $n = 1.8$ when the first monolayer is intercalated. Proton diffusion then occurs through an ordered array of hydrogen-bonded water molecules and room-temperature conductivity reaches $10^{-2}\ \Omega^{-1}\ cm^{-1}$. The temperature dependence of conductivity follows two different Arrhenius behaviors with a kink around 260 K. This corresponds to the freezing point of interlamellar water. The corresponding activation energies for proton conduction are 0.35 and 0.42 eV above and

(94) Szörényi, T.; Bali, K.; Hevesi, I. *J. Phys. (Paris)* **1985**, *46*, 473.
(95) Kiss, L. B.; Bali, K.; Szörényi, T.; Hevesi, I. *Solid State Commun.* **1986**, *58*, 609.
(96) Szörényi, T.; Bali, K.; Török, M. I.; Hevesi, I. *Thin Solid Films* **1984**, *121*, 29.
(97) Livage, J. Better Ceramics through Chemistry. *Mater. Res. Soc. Symp. Proc.* **1984**, *32*, 125.
(98) Livage, J.; Jolivet, J. P.; Tronc, E. *J. Non-Cryst. Solids* **1990**, *121*, 35.
(99) Austin, I. G.; Mott, N. F. *Adv. Phys.* **1968**, *18*, 41.
(100) Kounavis, P.; Vomvas, A.; Mytilineou, E.; Roilos, M.; Murawski, L. *J. Phys.: Solid State Phys.* **1988**, *21*, 967.
(101) Bullot, J.; Gallais, O.; Gauthier, M.; Livage, J. *Appl. Phys. Lett.* **1980**, *36*, 986.
(102) Bullot, J.; Cordier, P.; Gallais, O.; Gauthier, M.; Livage, J. *Phys. Status Solidi a* **1981**, *68*, 357.
(103) Bullot, J.; Cordier, P.; Gallais, O.; Gauthier, M.; Livage, J. *J. Non-Cryst. Solids* **1984**, *68*, 123.
(104) Murawski, L.; Gzowski, O.; Barboux, P.; Livage, J. *Thin Solid Films* **1988**, *167*, 67.
(105) Triberis, G. P. *J. Non-Cryst. Solids* **1988**, *104*, 135.
(106) Bullot, J.; Cordier, P.; Gallais, O.; Gauthier, M.; Babonneau, F. *J. Non-Cryst. Solids* **1984**, *68*, 135.
(107) Barboux, P.; Baffier, N.; Morineau, R.; Livage, J. *Solid State Ionics* **1983**, *9–10*, 1073.

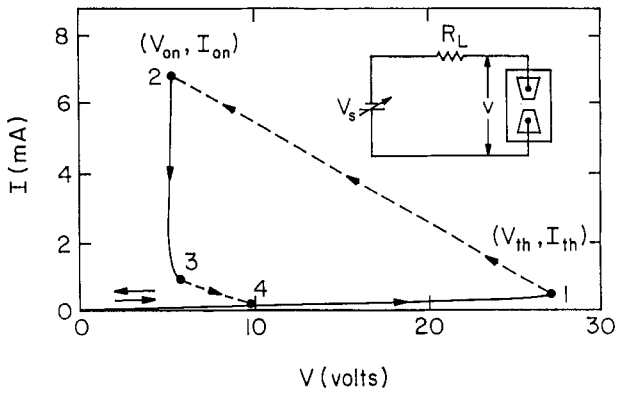

Figure 19. $I = f(V)$ characteristic of a switching device based on a $V_2O_5 \cdot 1.8H_2O$ layer according to ref 111.

below 260 K, respectively. For larger water content ($n > 1.8$) proton conduction becomes similar to that of an acid aqueous solution. It decreases as the pH increases, i.e., as more water is added to the gel.

Humidity sensors have been recently made with vanadium pentoxide based binary amorphous oxides V_2O_5–M_xO_y (M_xO_y = Ag_2O, Li_2O, SiO_2, GeO_2).[108] These materials were synthesized by the melt-quenching technique and dissolved in water in order to obtain colloidal solutions. These sols are then deposited onto a substrate giving thin films with a layered structure. Their transmittance and dc conductivity vary with humidity. These inorganic films can be combined with an organic polymer ([(hydroxypropyl)methyl]cellulose) by adding an aqueous solution to the organic polymer and depositing the solution onto a substrate. Hybrid films work very well as highly sensitive humidity sensors. Their impedance decreases by 2 orders of magnitude when the relative humidity increases from 80% to 97%.[108]

Two-terminal switching devices based on $V_2O_5 \cdot nH_2O$ gels have been patented.[109] Reversible switching between "on" and "off" states occurs on the timescale of microseconds and leads to a change in the electrical conductance (dI/dV) of 2 orders of magnitude (Figure 19).[110] However, switching is never observed unless the device is first overbiased to a value about twice the switching voltage, i.e., around 50 V. A narrow filament about 10 μm wide then appears to be formed in the gap between electrodes and can be seen by optical microscopy.[111] This filament undergoes a metal–insulator transition around 60 °C as for nonstoichiometric VO_{2-x}. Such behavior arises from the electrochemical reduction of vanadium ions in the $V_2O_5 \cdot nH_2O$ gel when a dc voltage is applied. This leads to the formation of a VO_2 filament growing from the cathode to the anode. The switching phenomenon is then associated with an electrothermally driven metal–insulator transition in the channel.

Vanadium dioxide thin films have been grown from vanadium(IV) alkoxides.[112,113] They are annealed under nitrogen at 600 °C to form polycrystalline VO_2. These gel-derived VO_2 films undergo a reversible semiconductor–metal phase transition near 72 °C. The electrical resistance decreases by 1 or 2 orders of magnitude and the near infrared transmittance approaches zero as the material undergoes this phase transition. VO_2 films have been doped with hexavalent cations by combining isopropanolic solutions of vanadium tetrakis(*tert*-butoxide) with those of $MOCl_4$ (M = Mo^{6+}, W^{6+}) in order to lower the transition temperature.[114]

b. Ion Exchange and Intercalation. Vanadium pentoxide gels have a layered structure.[59] They are able to intercalate a wide variety of inorganic and organic guest species.[115] Water adsorption and dissociation occurs at the oxide–water interface leading to the formation of surface hydroxyl groups. However such OH groups are known to exhibit acid or basic properties. This behavior depends on electron transfer within the V–OH bond. V(V) is a highly charged cation so that acid dissociation occurs as follows:

$$-V-OH + H_2O \rightarrow -V-O^- + H_3O^+$$

This accounts for the acid properties of the gel that could be described as $V_2O_5 \cdot 0.3(H_3O^+)1.5(H_2O)$. Intercalation mainly involves proton-exchange reactions with the acidic protons of the gel. The pH of the solution increases, and the basal distance between layers varies.[116] Some redox reactions also occur, leading to the formation of V(IV) ions in the V_2O_5 matrix.[117] Reduction must be limited, otherwise flocculation occurs and intercalation is no more reversible.[118] The nature of these redox reactions is not yet clearly established. Vanadium reduction is probably due to anionic species. It has also been postulated that hydroxyl groups could be involved in a redox process favored by the elimination of water molecules under vacuum or upon heating.[119] Vanadium reduction would then occur at the same time as guest species are deprotonated.

Intercalation in V_2O_5 gels is much easier than with usual crystalline layered lattices. It occurs readily at room temperature within a few minutes as soon as the gel is dipped into the solution of ionic salts.[120] The internal structure of the oxide network and the 1-D stacking of the V_2O_5 ribbons are not destroyed. The basal distance increases and intercalation can be easily followed by X-ray diffraction.[115]

Intercalation of Metal Cations. Chemical titration shows that the exchange capacity of vanadium pentoxide gels for monovalent metal cations M^+ is close to 1.75 mequiv/g, i.e., 0.3 equiv/V_2O_5.[119–121] This value corresponds to the number of acid protons previously measured by protometric titration. The rate of ionic H^+/M^+ exchange is mainly controlled by ion diffusion through the gel. Proton diffusion coefficients are of about $D = 1.6 \times 10^{-8}$ cm^2 s^{-1}.[122] Large monovalent metal cations are usually intercalated with one water layer leading to a basal distance around $d = 11$ Å, while smaller polyvalent cations are intercalated with two water layers with d close to 13.6 Å. This results from the competition between two energy

(108) Inubushi, A.; Masuda, S.; Okubo, M.; Matsumoto, A.; Sadamura, H.; Suzuki, K. In *High Tech Ceramics*; Vincenzini, P., Ed.; Elsevier Science: Amsterdam, 1987; p 2165.
(109) Bullot, J.; Livage, J. French Patent 8,113,665, 1981.
(110) Bullot, J.; Gallais, O.; Gauthier, M.; Livage, J. *Phys. Status Solidi a* **1982**, *71*, K1.
(111) Zhang, J. G.; Eklund, P. C. *J. Appl. Phys.* **1988**, *64*, 729.
(112) Speck, K. R.; Hu, H. S. W.; Sherwin, M. E.; Potember, R. S. *Thin Solid Films* **1988**, *165*, 317.
(113) Speck, K. R.; Hu, H. S. W.; Murphy, R. A.; Potember, R. S. *Mater. Res. Soc. Symp. Proc.* **1988**, *121*, 667.
(114) Potember, R. S.; Speck, K. R. Better Ceramics through Chemistry IV. *Mater. Res. Symp. Proc.* **1990**; *180*, 753.
(115) Aldebert, P.; Baffier, N.; Legendre, J. J.; Livage, J. *Rev. Chim. Miner.* **1982**, *19*, 485.
(116) Ruiz-Hitzky, E.; Casal, B. *J. Chem. Soc., Faraday Trans. 1*, **1986**, *82*, 1597.
(117) Aldebert, P.; Paul-Boncour, V. *Mater. Res. Bull.* **1983**, *18*, 1263.
(118) Van Damme, H.; Letellier, M.; Tinet, D.; Kihal, B.; Erre, R. *Mater. Res. Bull.* **1984**, *19*, 1635.
(119) Znaidi, L.; Baffier, N.; Huber, M. *Mater. Res. Bull.* **1989**, *24*, 1501.
(120) Bouhaouss, A.; Aldebert, P.; Baffier, N.; Livage, J. *Rev. Chim. Miner.* **1985**, *22*, 417.
(121) Baffier, N.; Znaidi, L.; Huber, M. *Mater. Res. Bull.* **1990**, *25*, 705.
(122) Znaidi, L.; Baffier, N.; Lemordant, D. *Solid State Ionics* **1988**, *28–30*, 1750.

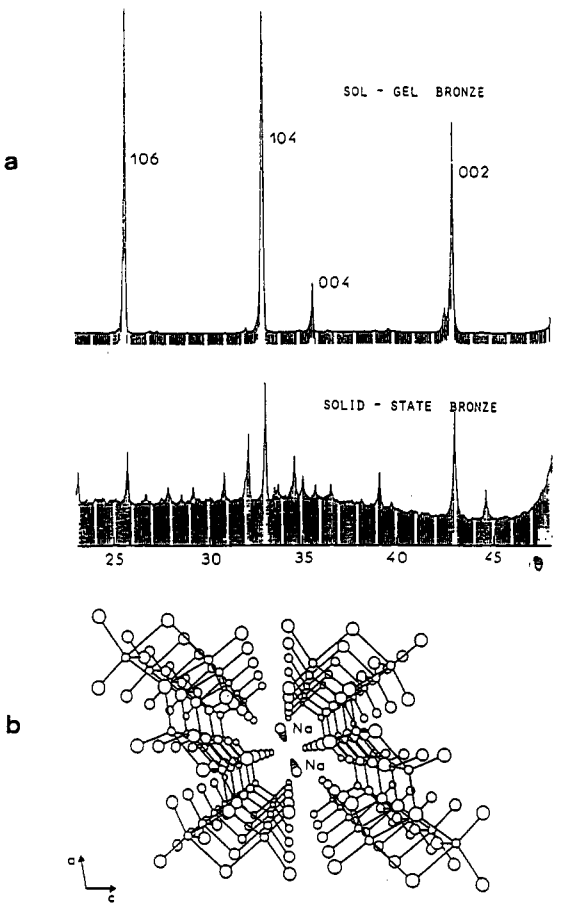

Figure 20. Anisotropic $\beta Na_{0.33}V_2O_5$ layers made from vanadium pentoxide gels: (a) X-ray diffraction pattern of sol–gel and solid-state bronzes. (b) Structure showing the tunnels perpendicular to the substrate.

terms:[120] (i) The energy required to separate V_2O_5 layers, which increases with Δd. (ii) The solvation energy of the cation which increases with the charge/radius ratio (Z/r). A linear empirical relationship between the hydration number n and the field strength Z/r was proposed recently.[123] According to these data, the limit between mono- and bilayer intercalation roughly corresponds to Z/r = 16.7 e Å^{-1}. These observations have been extended to the solvation of intercalated metal cations by organic solvents.[124]

The ordered stacking of V_2O_5 layers deposited from gels is preserved not only upon intercalation of metal cations but also during a thermal treatment. Anisotropic coatings of vanadium bronzes β-$Na_{0.33}V_2O_5$ were made upon heating vanadium pentoxide gels in which Na^+ ions were intercalated.[119] These sol–gel bronzes crystallize above 400 °C and exhibit the same monoclinic structure as the usual vanadium bronzes obtained via conventional solid-state reactions at 600 °C.[5,125] However X-ray diffraction suggests that (a,c) planes are preferentially oriented parallel to the substrate (Figure 20a).[119] The tunnels of the bronze structure remain perpendicular to the substrate and ion exchange with the solution becomes easier (Figure 20b).[125,126] Anisotropic sol–gel bronzes therefore exhibit

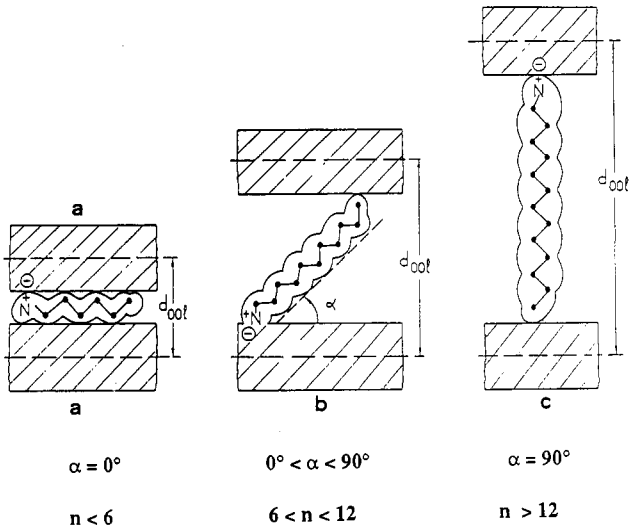

Figure 21. Orientation of alkylammonium chains $[C_nH_{2n+1}N(CH_3)_3]^+$ between V_2O_5 layers deduced from X-ray diffraction experiments.

very interesting properties as reversible cathodes for lithium batteries. They offer a better reversibility and a larger capacity toward Li^+ insertion.[126] Similar alkali-metal-containing hydrated vanadium oxides with layered structures have been obtained recently by the hydrothermal treatment of $VOSO_4$ aqueous solutions. The anisotropic structure is also preserved upon heating leading to vanadium oxide phases with different basal distances.[128,129]

Ionic intercalation with large polycations leads to the formation of pillared vanadium oxide gels similar to the well-known "pillared clays".[130] These new layered materials were prepared via a double ion-exchange process. The basal distance between V_2O_5 layers is first increased via the intercalation of cations such as VO^{2+} solvated with two water layers. The well-known $[Al_{13}O_4(OH)_{24}(H_2O)_{12}]^{7+}$ polycation can then be intercalated easily. The basal distance increases up to 18 Å, and the nitrogen BET surface area becomes larger than 80 m^2/g. Similar results were obtained with smaller polycations $[M_6Cl_8(OH)_n(H_2O)_m]^{(4-n)+}$ (M = Mo, W) by using a single exchange process.[130]

Intercalation of Molecular Species. Molecular species can also be intercalated into V_2O_5 gels. At room temperature, intercalation proceeds mainly through proton-transfer reactions involving protons from the poly(vanadic acid) gel. Molecular ions such as cobaltocenium $(CoCp_2)^+$ or ferrocenium $(FeCp_2)^+$,[117] long-chain alkylammonium $[C_nH_{2n+1}N(CH_3)_3]^+$),[131] nitrogenated bases (pyridine, pyrazine),[132] and even viologens[133,134] have been intercalated into the layered structure of vanadium pentoxide gels.[175] The orientation of these molecular species between oxide layers is deduced from the basal distance d measured from X-ray diffraction data. The angle α

(123) Baffier, N.; Znaidi, L.; Badot, J. C. *J. Chem. Soc., Faraday Trans.* **1990**, *86*, 2623.
(124) Lemordant, D.; Bouhaouss, A.; Aldebert, P.; Baffier, N. *Mater. Res. Bull.* **1986**, *21*, 273.
(125) Badot, J. C.; Gourier, D.; Bourdeau, F.; Baffier, N.; Tabuteau, A. *J. Solid State Chem.* **1991**, *92*, 8.
(126) Pereira-Ramos, J. P.; Messina, R.; Znaidi, L.; Baffier, N. *Solid State Ionics* **1988**, *28–30*, 886.
(127) Bach, S.; Baffier, N.; Pereira-Ramos, J. P.; Messina, R. *Solid State Ionics* **1989**, *37*, 41.
(128) Oka, Y.; Yamamoto, N.; Ohtani, T.; Takada, T. *Nippon Seramikkusu Kyokai Gakujutsu Ronbunshi* **1989**, *97*, 1441.
(129) Oka, Y.; Yao, T.; Yamamoto, N. *Nippon Seramikkusu Kyokai Gakujutsu Ronbunshi* **1990**, *98*, 1365.
(130) Khairy, M.; Tinet, D.; Van Damme, H. *Chem. Commun.*, in press.
(131) Bouhaouss, A.; Aldebert, P. *Mater. Res. Bull.* **1983**, *18*, 1247.
(132) Casal, B.; Ruiz-Hitzky, E.; Crespin, M.; Tinet, D.; Galvan, J. C. *J. Chem. Soc., Far. Trans. 1* **1989**, *86*, 4167.
(133) Nakato, T.; Kato, I.; Kuroda, K.; Kato, C. *J. Colloid Interface Sci.* **1989**, *133*, 447.
(134) Kato, I.; Nakato, T. Kuroda, K.; Kato, C. *Colloids Surf.* **1990**, *49*, 241.

between alkyl chains and oxide layers for instance can be determined by plotting d as a function of the number n of carbon atoms in the alkyl chain (Figure 21). The orientation of alkylammonium ions depends on electrostatic interactions between oxide layers and van der Waals attractions between alkyl chains. Small alkylammonium ions ($n < 6$) lie parallel to the layer planes while long chain ions ($n > 12$) remain parallel to each others and perpendicular to V_2O_5 layers.[131]

Polar organic solvents can also be intercalated into V_2O_5 gels.[135] They lead to a swelling of the gel and an increase of the basal distance between oxide layers. Depending on the nature of the organic molecule, different processes such as redox reactions, protonation, or dipolar adsorption are involved in these intercalation reactions. It is therefore rather difficult to predict whether a given organic molecule would intercalate or not. Neither dipolar moments nor relative permittivities or Gutman's donor numbers allow any reproducible prediction. Actually all interactions have to be taken into account and it was suggested that the Hildebrand solubility parameter δ (square root of the cohesive energy density) could provide a rather convenient parameter. According to the authors, intercalation is usually not observed when $\delta < 13$ cal$^{1/2}$ cm$^{-3/2}$.[136]

Molecular bronzes have been synthesized via the redox intercalation of organic molecules in V_2O_5 gels.[137,138] The reaction of TTF, for instance, results in a charge transfer toward the oxide phase and an amorphization of the gel. This reaction is not reversible and should be described as a redox reaction rather than intercalation. According to the authors, a new crystalline phase is obtained for TTF/V_2O_5 molar ratio larger than 0.35. No single crystal can be obtained, so that its structure has not been determined. Such molecular bronzes exhibit both proton and electron conduction.[138]

The in situ intercalation/polymerization of organic monomers such as aniline, pyrrole, and 2,2'-bithiophene yields layered materials containing monolayers of conductive polymers in the intralamellar space of vanadium oxide gels.[139,140] The driving force for intercalation is based on the high redox potential of $V_2O_5 \cdot nH_2O$ gels. The vanadium oxide network is reduced to form V(IV) centers, and organic monomers are oxidatively polymerized into electrically conductive polymers. This results in new molecular composites of two electrically active but chemically diverse components: organic conductive polymers and inorganic vanadium bronzes.[141] Such materials are highly conductive. The room-temperature conductivity of polythiophene intercalated gels, $[(C_8H_4S_2)_{0.44}-V_2O_5 \cdot 0.54H_2O]$ for instance, is as high as 0.1 Ω^{-1} cm^{-1}. Black shiny products are obtained as powders or free-standing flexible films.[142] The layered turbostratic structure of V_2O_5 gels is preserved (Figure 22) so that these materials could provide theoretical models for oriented polymers.[139] This could be a major advance if we keep in mind that only insoluble amorphous powders are actually obtained by

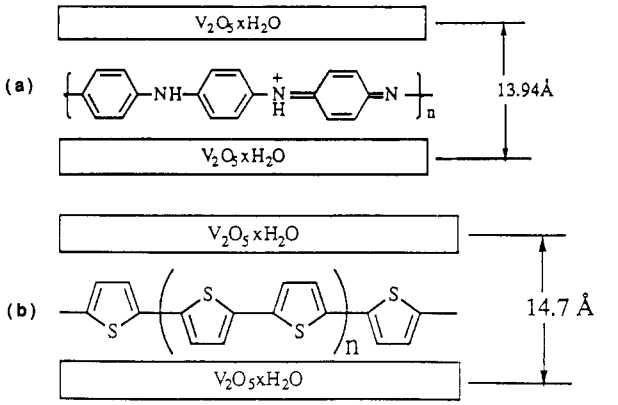

Figure 22. Suggested structure of polymer bronzes made via the in situ intercalation/polymerization of organic monomers in $V_2O_5 \cdot nH_2O$ gels according to 139–142.

usual electrochemical or chemical oxidation of the corresponding monomers.

c. Electrochemical Properties. Ion-insertion materials have been extensively studied for their potential application as reversible cathodes in lithium batteries. However such compounds cannot be really useful as positive electrodes unless the free energy of the reduction process is very negative and the maximum reversible intercalation rate remains high.[143]

Vanadium pentoxide V_2O_5 would be one of the promising candidates since its redox potential is higher than 3 V with reference to lithium. It offers stoichiometric energy densities as high as 600 W h kg^{-1}.[144] Electrochemical lithium insertion occurs together with compensating electrons leading to the formation of vanadium bronzes as follows:

$$V_2O_5 + xLi^+ + xe^- \leftrightarrow Li_xV_2O_5$$

Electroreduction occurs in four steps with an overall balance close to 3e/mol of oxide. However, despite its layered structure, the crystalline oxide behaves as a 3-D framework rather than a van der Waals host and reversible lithium insertion remains limited to the two first steps ($x < 1$).[145]

Higher Li^+ diffusion rates and better reversibility are observed with vanadate glasses.[146] Structural changes are limited, and reversibility up to $x = 1.8$ was reported for amorphous V_2O_5. The open-circuit voltage continuously decreases showing that no phase transition occurs in the 3.5–2-V (vs Li/Li^+) potential range.[147]

Reversible electrochemical insertion of Li^+ ions into the layered structre of $V_2O_5 \cdot 1.6H_2O$ gels was reported a few years ago.[148] Experiments were performed in a propylene carbonate solution so that an exchange of water molecules by the organic solvent was first observed even in the absence of any applied voltage leading to a larger basal distance $d = 21.5$ Å. The 1-D stacking of oxide ribbons then appears to be progressively destroyed during electrochemical Li^+ insertion as the amount of reduced vanadium ions increases (Figure 23). However the turbos-

(135) Aldebert, P.; Baffier, N.; Gharbi, N.; Livage, J. *Mater. Res. Bull.* **1981**, *16*, 949.
(136) Lemordant, D.; Bouhaouss, A.; Aldebert, P.; Baffier, N. *J. Chim. Phys.* **1986**, *83*, 105.
(137) Masbah, H.; Tinet, D.; Crespin, M.; Erre, R.; Setton, R.; Van Damme, H. *Chem. Commun.* **1985**, 935.
(138) Erre, R.; Masbah, H.; Crespin, M.; Van Damme, H.; Tinet, D. *Solid State Ionics* **1990**, *37*, 239.
(139) Kanatzidis, M. G.; Wu, C.-G. *J. Am. Chem. Soc.* **1989**, *111*, 4139.
(140) Kanatzidis, M. G.; Wu, C.-G.; Marcy, H. O.; DeGroot, D. C.; Kannewurf, C. R. *Chem. Mater.* **1990**, *2*, 222.
(141) Wu, C.-G.; Kanatzidis, M. G.; Marcy, H. O.; DeGroot, D. C.; Kannewurf, C. R.; *Polym. Mater. Sci. Eng.* **1989**, *61*, 969.
(142) Kanatzidis, M. G.; Wu, C.-G.; Marcy, H. O.; DeGroot, D. C.; Kannewurf, C. R. *Chem. Mater.*, in press.
(143) Whittingham, M. S. *Prog. Solid State Chem.* **1978**, *12*, 41.
(144) West, K.; Zachau-Christiansen, B.; Ostergard, M. J. L.; Jacobsen, T. *J. Power Sources* **1987**, *20*, 165.
(145) Farcy, J.; Messina, R.; Perichon, J. *J. Electrochem. Soc.* **1990**, *137*, 1337.
(146) Machida, N.; Fuchida, R.; Minami, T. *J. Electrochem. Soc.* **1989**, *136*, 2133.
(147) Nabavi, M.; Sanchez, C.; Taulelle, F.; Livage, J.; de Guibert, A. *Solid State Ionics* **1988**, *28–30*, 1183.
(148) Araki, B.; Mailhé, C.; Baffier, N.; Livage, J.; Vedel, J. *Solid State Ionics* **1983**, *9–10*, 439.

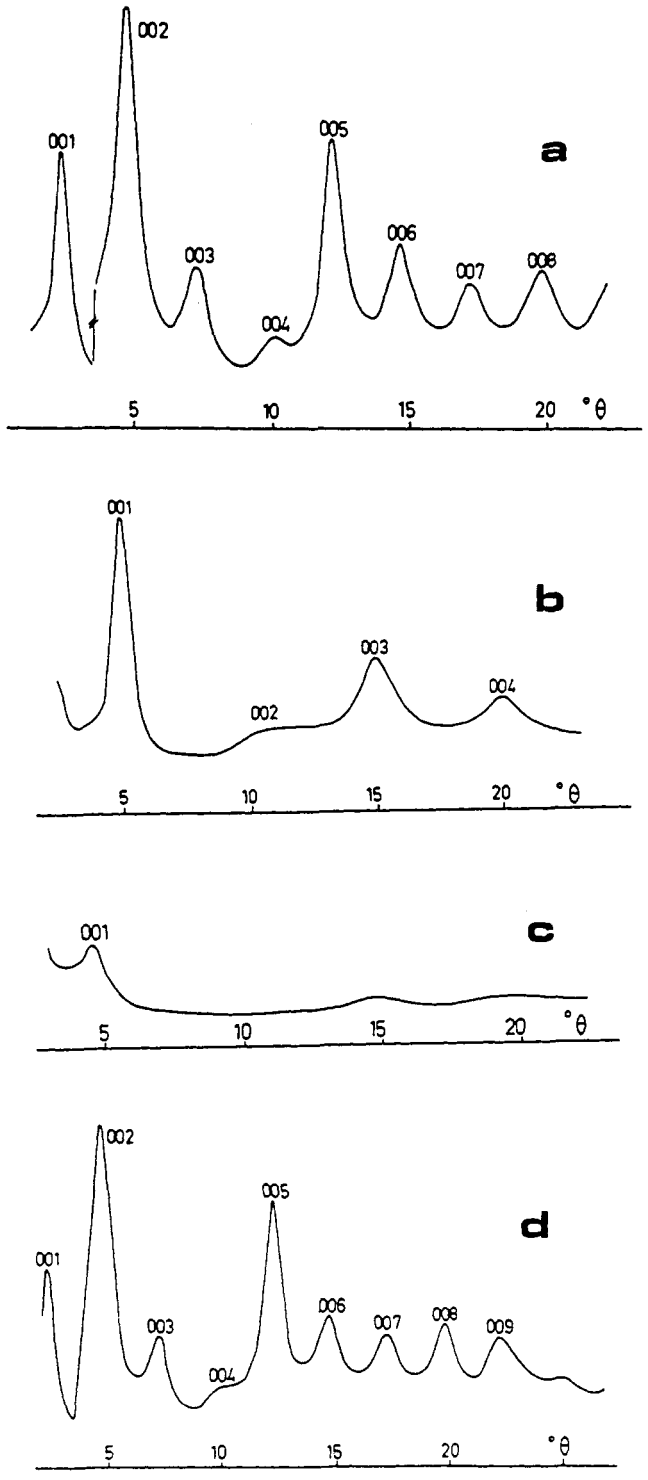

Figure 23. Modification of the X-ray diffraction pattern of a vanadium pentoxide gel as a function of the amount x of electrochemically inserted Li^+: $x = 0.1$ (a), $x = 1.1$ (b), $x = 1.6$ (c), $x = 0.1$ after reversible oxidation (d).

tatic stacking of the gel is restored upon electrochemical oxidation at least during the first cycles. Two steps are observed on the open-circuit voltage curve. They correspond to $Li_xV_2O_5$ phases with $x = 1.1$ and $x = 1.6$ respectively.[148]

The behavior of $V_2O_5 \cdot nH_2O$ xerogels as reversible cathodes in lithium cells was studied by several groups with different materials and different cell configurations so that results are hardly comparable. Continuous discharge curves are reported by some authors, while others observe several steps. These discrepancies seem to be related to

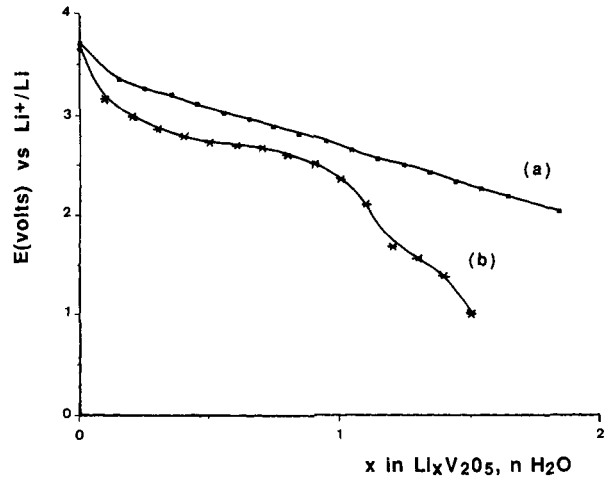

Figure 24. Open-circuit discharge curves of $V_2O_5 \cdot nH_2O$ xerogels in $Li/LiClO_4$–PEO/V_2O_5 cells: (a) $n = 0.3$; (b) $n = 1.8$.

the hydration state of vanadium pentoxide gels ranging from $n = 0.3$ up to $n = 2.2$. The presence of water or other solvent molecules in the gel leads to a more ordered stacking of V_2O_5 ribbons. Orientated gels give sharp $00l$ X-ray diffraction patterns and behave almost as crystalline materials. Lithium insertion leads to well-defined steps that can be seen on discharge curves or cyclic voltammetry experiments (Figure 24).

Vanadium pentoxide gels $V_2O_5 \cdot 1.6H_2O$, prepared from decavanadic acid, were deposited as a thin film (about 5 μm thick) onto a platinum disk. This electrode was then dipped into a $LiClO_4$ solution in propylene carbonate. All exchangeable water molecules and about $0.3H_3O^+$ per V_2O_5 were thus removed before electrochemical experiments leading to a basal spacing $d = 21.6$ Å.[149] The electrochemical behavior of this xerogel is typical of an amorphous compound with an open circuit voltage at $x = 0$ higher than that of orthorhombic V_2O_5 and a continuous voltage decrease between 3.5 and 2 V (vs Li/Li^+). The reversibility of lithium insertion appears to be rather good as 40% of the initial capacity is still obtained after 10 cycles. According to the authors the main advantages of this xerogel would be the possibility to have a single-step reduction process centered around 3 V and a faradic capacity (250 A h kg^{-1}), almost twice that of crystalline V_2O_5. Better electrochemical results can be obtained when graphite is mixed to the V_2O_5 xerogel in order to improve its electronic conductivity.[149]

The electrochemical behavior of more dehydrated $V_2O_5 \cdot 0.1H_2O$ xerogels heated at 230 °C was studied by using $LiCF_3SO_3$ in PEO (poly(ethylene oxide)) as an electrolyte.[144] The discharge curve was also nearly linear between 3.5 and 2.2 V. Reversibility remains good, but the energy density is not as high as expected (420 W h kg^{-1} for $x = 1.1$). In these experiments a polymeric electrolyte was used in order to prevent the intercalation of organic solvents into the gel. However, according to the authors apparent inconsistencies in the experiments seem to be due to the formation of a PEO–V_2O_5 compound with a layer spacing $d = 13.4$ Å. This solvate or intercalation compound is formed during the preparation of the composite electrode.[144]

Two inflection points around $x = 0.27$ and $x = 0.44$ were observed by galvanostatic intermittent titration with a $V_2O_5 \cdot 2.2H_2O$ xerogel.[150] Propylene carbonate is co-in-

(149) Baddour, R.; Peira-Ramos, J. P.; Messina, R.; Perichon, J. *J. Electroanal. Chem.* **1990**, *277*, 359.

tercalated with Li^+, but interlamellar water still remains in the xerogel. The basal distance decreases slightly with x, and the layered structure of V_2O_5 ribbons is gradually destroyed.[151] Similar experiments were also performed using LiI in acetonitrile as an electrolyte.[152] Infrared absorption shows that oxygen atoms belonging to interlamellar water molecules and the oxide ribbons coordinate competitively toward inserted Li^+ ions when $x < 0.15$. No more water is available beyond this value.[153] Both an abrupt decrease of the basal distance and the disappearance of hydrogen bonds between water and V=O sites are observed around $x = 0.15$ where the open-circuit voltage exhibits an inflection point.[152]

The electrochemical behavior of vanadium pentoxide gels synthesized from alkoxides depends on the hydrolysis ratio $h = H_2O/V_2O_5$.[38] Orange gels hydrolyzed with $h = 3$ still contain organic groups bonded to the oxide network. They behave like amorphous materials, and the open-circuit voltage decreases continuously. Reversible electrochemical Li^+ insertion is also observed with red gels hydrolyzed with a large excess of water ($h = 100$). However, several reduction and oxidation steps are observed on cyclic voltammetry curves suggesting the presence of well-defined insertion sites. Some steps are also observed on the discharge curve of the $V_2O_5 \cdot 1.8H_2O$ xerogel recorded with a buttom cell containing PEO–$LiClO_4$ as an electrolyte (Figure 24).[38]

Vanadium pentoxide gels and mixed V_2O_5–TiO_2 gels have been studied recently as lithium insertion electrodes in polymeric electrolyte cells.[154,155] Addition of TiO_2 prevents the crystallization of vanadium oxide. These gels were shown to have gravimetric capacities similar to but higher rate capabilities than the well-known V_6O_{13}. According to the authors this could be due to the smaller size of oxide particles and their better dispersion in the acetylene black/PEO binder.[156]

Anisotropic $\beta Na_{0.33}V_2O_5$ bronzes prepared via the sol–gel route exhibit enhanced electrochemical properties.[157] Four well-defined Li^+ insertion processes are seen on the discharge curve between 3.5 and 2 V vs Li/Li^+. About 70% of the initial capacity is still recovered up to $x = 1.7$ after 80 cycles at 150 °C in DMSO.[126] Such a high reversibility must be related to the anisotropy of the electrode prepared from $V_2O_5 \cdot nH_2O$ gels.[121] Interesting results have also been obtained for the electrochemical insertion of Na^+ in such bronzes with a maximum uptake of 1.6 Na^+/mol of bronze.[127]

Electrochromic Devices. The electrochromic properties of transition-metal oxides have been extensively studied during the past two decades.[158] The best investigated and the most common oxide is WO_3. It turns reversibly from white to blue upon electrochemical reduction. Amorphous WO_3 thin films have already been used for electrochromic display devices, rearview mirrors, or smart windows.[159]

Vanadium pentoxide seems to be rather appropriate for lithium-based electrochromic systems. Sputtered V_2O_5 films exhibit a combination of anodic and cathodic colorations, the relative magnitudes of which depend on the thickness of the film and the amount of inserted Li^+.[160] Electrochromic V_2O_5 films have been synthesized via the sol–gel route, either from poly(vanadic acid) or from alkoxides.[161,162] Uniform and adherent films have also been deposited onto electroconductive glasses (ITO) by electrolyzing colloidal V_2O_5 aqueous solutions.[163,164] Color changes are rather weak and V_2O_5 thin films have been used as transparent counter electrodes for electrochromic devices.[165,166] However color changes can be seen on thicker films, which turn reversibly from orange on anodic polarization to green on cathodic polarization. Three colors devices (red–yellow–green) can even be obtained with thick films.[162] The response time of these electrochromic films ranges between 2 and 20 s depending on the applied voltage. Reversibility is rather good as optical switching is still observed after 8×10^4 cycles in a $LiClO_4$–propylene carbonate electrolyte.

Hybrid organic–inorganic thin films have been prepared from aqueous solutions containing vanadium pentoxide based binary sols, organic polymers, and dyes. They appear to be quite promising as an optical memory medium.[167] Binary oxides were made by the melt-quenching technique. The optical recording media are prepared by dissolving some organic polymers ([(hydroxypropyl)-methyl]cellulose) and dyes (4-formyl-*m*-benzenedisulfonic acid with N-ethyl-N-phenylbenzylamine) in a $(V_2O_5)_{0.75}$-$(GeO_2)_{0.25}$ sol. The solution is deposited onto a glass or plastic disk by spin-coating. The film is then heated at 100 °C for 30 min. X-ray diffraction gives a basal spacing of 22 Å, showing that organic additives are intercalated between the oxide layers. A Bi–Pb reflector layer about 500 Å in thickness is deposited onto the substrate by vacuum evaporation. These hybrid optical disks belong to the bubble-forming type of media. They have a high thermal response in which the surface of the film rises to give a small bubble under exposure to diode laser, He–Ne laser, electronic flash light, or electron beam.[167]

New composite polymeric materials have been recently synthesized via the sol–gel route.[168] A PPV (poly(*p*-phenylenevinylidene)) polymer precursor is homogeneously mixed with vanadic acid up to 50% by weight. A film is then cast, and during the heat treatment the polymer precursor converts into the final conjugated nonlinear optical polymer. The composite films show highly improved optical quality with large third-order nonlinear optical coefficient. According to the authors optical waveguiding have already been achieved through such films.[168]

d. Catalytic Properties. The catalytic properties of V_2O_5 are well-known. Considerable effort has been ex-

(150) Miura, T.; Sugiura, E.; Kishi, T.; Nagai, T. *Denki Kagaku* **1988**, *56*, 413.
(151) Miura, T.; Kunihiro, S.; Muranushi, Y.; Kishi, T. *Denki Kagaku* **1989**, *57*, 393.
(152) Miura, T.; Kanamori, N.; Muranushi, Y.; Kishi, T. *Denki Kanaku* **1989**, *57*, 29.
(153) Miura, T.; Kanamori, N.; Muranushi, Y.; Kishi, T. *Denki Kagaku* **1989**, *57*, 33.
(154) Minett, M. G.; Owen, J. R. *J. Power Sources* **1989**, *26*, 475.
(155) Minett, M. G.; Owen, J. R. *J. Power Sources* **1989**, *28*, 397.
(156) Minett, M. G.; Owen, J. R. *J. Power Sources* **1990**, *32*, 81.
(157) Pereira-Ramos, J. P.; Messina, R.; Bach, S.; Baffier, N. *Solid State Ionics* **1990**, *40–41*, 970.
(158) Colton, R. J.; Guzman, A. M.; Rabalais, J. W. *Acc. Chem. Res.* **1978**, *11*, 170.
(159) Bange, K.; Gambke, T. *Adv. Mater.* **1990**, *2*, 10.
(160) Cogan, S. F.; Nguyen, N. M.; Perrotti, J.; Rauh, R. D. *J. Appl. Phys.* **1989**, *66*, 1333.
(161) Yoshino, T.; Baba, N.; Kouda, Y. *Jpn. J. Appl. Phys.* **1987**, *26*, 782.
(162) Nabavi, M.; Doeuff, S.; Sanchez, C.; Livage, J. *Mater. Sci. Eng.* **1989**, *B3*, 203.
(163) Kouda, Y.; Yoshino, T.; Baba, N. *J. Chem. Soc. Jpn.* **1985**, 1050.
(164) Yoshino, T.; Baba, N.; Kouda, Y. *J. Surf. Sci. Soc. Jpn.* **1985**, *6*, 198.
(165) Andersson, A. M.; Granqvist, C. G.; Stevens, J. R. *Appl. Opt.* **1989**, *28*, 3295.
(166) Talledo, A.; Andersson, A. M.; Granqvist, C. G. *J. Mater. Res.* **1990**, *5*, 1253.
(167) Masuda, S.; Inubushi, A.; Okubo, M.; Matsumoto, A.; Sadamura, H.; Suzuki, K. In *High Tech Ceramics*; Vincenzini, P., Ed.; Elsevier Science: Amsterdam, 1987; p 2093.
(168) Prassad, P. N. Sol–gel optics. *SPIE* **1990**, *1328*, 168.

pended to develop methods for the uniform deposition of vanadium oxide as monolayers on support materials such as Al_2O_3, SiO_2, or TiO_2. It has even been shown that V_2O_5 supported on titanium dioxide exhibits a superior activity and selectivity in the selective oxidation of hydrocarbons.[169] Metavanadates, vanadium pentoxide, or vanadyl chlorides are currently used as impregnating agents. However, it is generally agreed that interactions of vanadia species with the supporting oxide are relatively weak. Therefore vanadium oxide particles tend to agglomerate upon heating, and the resulting catalysts are not stable toward high temperatures.

Interesting results were obtained by using vanadyl butoxide.[170,171] Oxide carriers were impregnated with a solution of $VO(O\text{-}i\text{-}Bu)_3$ in *n*-hexane. The selective reaction of the alkoxide with surface OH groups leads to the formation of single or double V_2O_5 layers at the surface of the oxide particles. Quantitative transformation of the surface hydroxyl groups into V=O species was found with Al_2O_3 and SiO_2 while only a fraction of these groups react with the vanadium alkoxide in the case of TiO_2 and MgO.[170] In general impregnation of acid carriers with V^{5+} increases the oxidizing character of the catalyst whereas the dehydration activity decreases.

Highly dispersed V_2O_5 particles in amorphous SiO_2 matrix were recently obtained via the sol–gel process.[172,173] Vanadia in these catalysts exhibit higher activity toward selective catalytic reduction and is considerably more stable against thermal aggregation than vanadia layers impregnated on silica supports. Mixed V_2O_5–SiO_2 gels were made via the hydrolysis and condensation of alkoxide precursors. Colloidal solutions are first prepared separately from $VO(O\text{-}i\text{-}Bu)_3$ and $Si(OEt)_4$ and then mixed and stirred together before drying and calcination. According to the authors, in all mixed-gel catalysts the well-dispersed vanadium oxide species are more stable than those in silica-supported vanadia layers.[172] The sol–gel process therefore appears promising for the synthesis of catalysts.

5. Conclusion

Transition-metal oxide gels have not yet received the attention they deserve. Vanadium pentoxide provides a significant example of their possibilities.

These gels can be synthesized from inorganic or metal-organic precursors and even from the molten oxide. Vanadium alkoxides are much more reactive than silicon alkoxides. The larger positive charge and coordination expansion of vanadium favor nucleophilic reactions such as hydrolysis, condensation, or complexation. It would therefore be interesting to control the sol–gel synthesis of V_2O_5 via the chemical modification of alkoxide precursors as was published for other transition metal alkoxides.[3] Hybrid organic–inorganic vanadium pentoxide gels could be synthesized. Attempts have been reported with the in situ intercalation and polymerization of organic molecules such as aniline or pyrrole. They lead to new molecular bronzes which exhibit high electrical conductivities.[138,139] Hybrid materials could also be synthesized in which organic groups would be directly bonded to vanadium.

The layered structure of vanadium pentoxide gels is specially interesting. It leads to the formation of ordered colloidal phases called tactoids. Anisotropic layers of large area can be easily deposited from such colloidal solutions. They behave as versatile host structures for the intercalation of ionic or molecular species allowing for instance the synthesis of anisotropic $\beta Na_{0.33}V_2O_5$ bronzes.[119] Nanocomposite materials similar to the well-known "pillared clays" could then be synthesized.[130] Moreover intercalated species appear to be oriented in the interlamellar space. Optically active organic molecules could be intercalated and oriented in layered gels in order to make nonlinear optical films.

Like many other transition-metal oxides, vanadium pentoxide is a mixed-valence compound. The amount of reduced V(IV) ions can be easily controlled via the sol–gel route in order to tailor the electronic properties of vanadium pentoxide gels. Semiconducting layers of large area are now currently used as antistatic coatings.[88] Mixed conduction properties arising from both electronic and ionic diffusion open new opportunities for microionic devices such as humidity sensors, microbatteries, or electrochromic displays. Patents and prototypes are available. Vanadium pentoxide gels could lead to industrial applications in the near future.

However, as for all other gels, vanadium pentoxide gels are very difficult to characterize accurately. Despite their layered structure, they are not really crystallized. Short-range order around vanadium atoms can be analyzed quite well by using spectroscopic techniques such as ^{51}V NMR or X-ray absorption. However little is known about long-range order. Small-angle scattering experiments give information on the size and shape of particles. They do not tell how atoms are distributed inside the oxide framework. Moreover the true chemical composition is not even obvious and these gels could be described as hydrous oxides as well as poly(vanadic acids). Therefore much work as still to be done before a real mastery of the sol–gel process could be reached.

Acknowledgment. I am very grateful to all my coworkers and mainly to those who made their Ph.D. on vanadium pentoxide gels: C. Sanchez, N. Gharbi, L. Nejem, F. Babonneau, O. Gallais, A. Bouhaouss, P. Aldebert, P. Barboux, J. C. Badot, L. Znaidi, and M. Nabavi.

Registry No. V_2O_5, 1314-62-1.

(169) Bond, G. C.; Sarkany, J.; Parfitt, G. O. *J. Catal.* **1979**, *57*, 476.
(170) Kijenski, J.; Baiker, A.; Glinski, M.; Dollenmeier, P.; Wokaun, A. *J. Catal.* **1986**, *101*, 1.
(171) Baiker, A.; Dollenmeier, P.; Glinski, M. *Appl. Catal.* **1987**, *35*, 365.
(172) Baiker, A.; Dollenmeier, P.; Glinski, M.; Reller, A.; Sharma, V. K. *J. Catal.* **1988**, *111*, 273.
(173) Wokaun, A.; Schraml, M. *J. Catal.* **1989**, *116*, 595.
(174) Kittaka, S.; Uchida, N.; Miyahara, H.; Yokora, Y. *Mater. Res. Bull.* **1991**, *26*, 391.
(175) Nakato, T.; Ise, T.; Sugahara, Y.; Kuroda, K.; Kato, C. *Mater. Res. Bull.* **1991**, *26*, 309.